Polymer Bulletin (2021) 78:4743–4777
https://doi.org/10.1007/s00289-020-03318-w

REVIEW PAPER

Polyaniline-TiO_2-based photocatalysts for dyes degradation

Nirmala Kumari Jangid, et al. *[full author details at the end of the article]*

Received: 20 March 2020 / Revised: 12 June 2020 / Accepted: 26 July 2020 / Published online: 7 August 2020

Abstract

For the last few decades, photocatalysis has attracted as an emerging successful technology for purifying wastewater by dye degradation from households and industries. TiO_2-based photocatalysis has gained wide attention due to its importance in energy source as well as its outstanding involvement in the reduction in environmental problems. Consequently, researchers and scientists are looking for the synthesis of polyaniline-TiO_2-based photocatalysts which are widely being used for the degradation of dyes. Lately, the use of polyaniline as photosensitizers has proved that it immensely enhances photodegradation by its excellent photocatalytic activity under both ultraviolet light and natural sunlight irradiation. Considering this most unique performance of Polyaniline-TiO_2-based photocatalysis, the present review provides the recent advances and trends in the development of ultraviolet and visible light-responsive polyaniline-TiO_2-based photocatalysis for their potential application in environmental remediation by dye degradation.

Graphic abstract

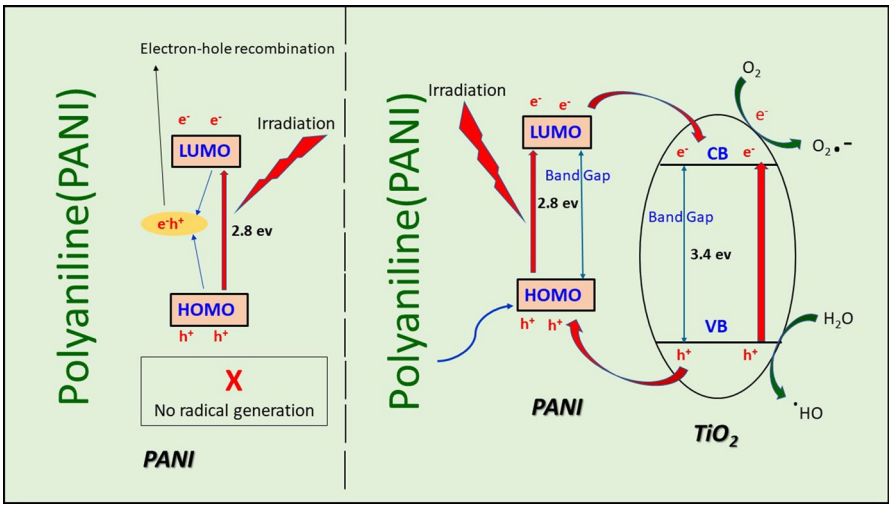

Keywords Polyaniline · Photocatalysis · TiO_2 · Organic pollutants · Methylene blue · Rhodamine B · Malachite green · Methylene orange

Abbreviations

NSA	Naphthalenesulfonic acid
APS	Ammonium persulphate
CB	Conduction band
CPs	Conducting polymers
CSA	Camphorsulfonic acid
HOMO	Highest occupied molecular orbital
HRP	Horseradish peroxidase
LUMO	Lowest unoccupied molecular orbital
MB	Methylene blue
MeO	Methyl orange
MG	Malachite green
NPs	Nanoparticles
PANI	Polyaniline
PET	Poly(ethyleneterephthalate)
PPy	Polypyrrole
PTh	Polythiophene
RB	Rhodamine B
RR45	Reactive red 45
SPS	Sulfonated polystyrene
THF	Tetrahydrofuran
UV	Ultraviolet
VB	Valance band

Introduction

Since the last few decades, organic synthetic dyes initiating from dye and textile industries, area-wide cause for environmental pollution. To terminate the possibility of water pollution, these dyes have been removed from wastewaters, via various techniques. Recently, organic pollutants have been effectively converted into harmless matter by using the method of photocatalytic degradation [1]. Photocatalysis has attracted much attention as it is one of the utmost auspicious advanced oxidation processes. Photocatalysis can be functioned at ambient temperature as well as mineralizes toxic organic compounds to carbon dioxide, water, and mineral acids [2]. For the treatment of wastewater, photocatalytic reaction illuminated with UV and visible light has gained much attention. Photocatalytic degradation of organic compounds by semiconducting materials such as Tin (IV) oxide [3], zinc oxide [4], titanium dioxide [5, 6], zirconium dioxide [7], iron (III) oxide [8], and cadmium sulfide [9] has been reported early.

Titanium dioxide, in the anatase form having nanosized, exhibits outstanding photocatalytic activity under ultraviolet irradiation [10]. It is one of the most frequently

used commercial photocatalysts, due to its advantageous properties such as low cost, non-toxicity, environment friendly, greater chemical stability for the oxidation of pollutants in air and water [11]. The utilization of photoanode of TiO_2 for solar energy conversion, photochemical water splitting has been studied by *Fujishima and Honda* [12, 13] Undesirable organic pollutants have been decomposed into the aqueous solution using photocatalysis [14]. Filtration, sedimentation, disinfection, and coagulation are the conventional methods through which the organic pollutants do not destroy completely [15–18]. The chemical and physical properties, as well as high surface activity of the TiO_2 photocatalysis, were utilized for the mineralization of dyes [19]. Anatase and rutile are the general forms of TiO_2 crystalline forms that have been studied extensively, and it has been observed that the anatase form is more active in comparison with rutile [20, 21]. Bandgap, structural properties, distribution of particle size, porosity, crystal defects, and density of surface hydroxyl are the properties on which the photocatalytic properties of TiO_2 depend [22]. The bandgap of TiO_2 has been observed to be 3.4 eV [23]. The surface area is directly associated with the effectiveness of a catalyst, and hence, it has been considered as a major parameter for efficient photocatalysis [24–27]. A possible mechanism of charge transfer and photocatalytic degradation of organic pollutants/dyes over the PANI/TiO_2 catalyst is shown in Fig. 1.

The electrons are excited from the valence band to the conduction band on the incident of the photon of light with energy equivalent or higher than the bandgap and results in the presence of free holes in the valence band. The energy in the form of the photon is released due to the recombination of these electrons and holes in a very small time [28–30]. Reduction reaction occurs with electron acceptors adsorbed by the surface on the migration of electrons and holes with higher energy

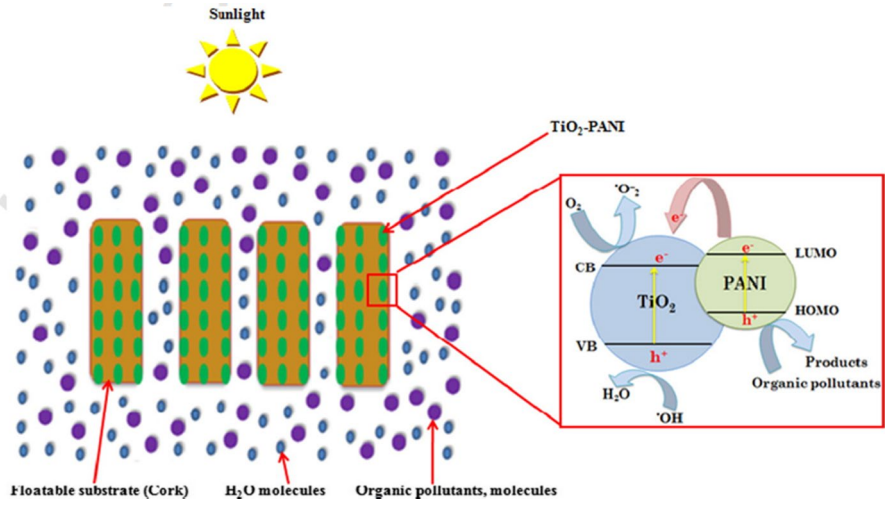

Fig. 1 Proposed mechanism of charge transfer on PANI/TiO_2 surface under sunlight irradiation. Reproduced from Journal of Environmental Sciences, vol. 60, TiO_2–PANI/Cork composite: A new floating photocatalyst forthe treatment of organic pollutants under sunlight irradiation, pp. 3–13, © 2017, with permission from Elsevier

to the catalyst's surface, while hydroxyl radicals have been produced on the reaction of holes with surface hydroxyls [31]. The extent of electrons and holes recombination enhances due to the increase in electrons in the conduction band if oxidation of pollutants and reduction in oxygen do not proceed simultaneously [32]. Though the relatively high bandgap limits its photocatalytic activity under visible light (Vis), however, its low quantum efficiency, resulting due to the recombination of holes and electrons, is an additional disadvantage of it. Therefore, the prevention of electron accumulation is highly important for effective photocatalytic oxidation. The fundamental photocatalytic mechanism has been constituted by these redox reactions [33].

Ultraviolet (UV) light which constitutes barely 3–5% of the solar spectrum has been used by these semiconductors which were responsible for its drawback and restricts the commercial application [34, 35]. The photocatalytic activity of these semiconductors can be enhanced by extending the light absorption of semiconductor materials toward visible regions by engineering the semiconductor's gap of the band [36]. Therefore, interest has been increased for the development of semiconductor materials with visible light. Noble metals doping, nonmetallic doping, and metal/nonmetal codoping are the various methods that are used for the development of visible light-responsive semiconductor materials [37]. Coupling of semiconductors of large bandgap with conducting polymers of small bandgap has been used as an alternative technique to increase the photocatalytic performance. As visible light cannot be absorbed by the wide bandgap, they can be "sensitized" by semiconductor materials with a narrow bandgap, and light is absorbed by the newly formed composite system in the visible region because of a strong coupling effect [38]. CPs consist of extended π–e^- system and suitable for semiconductors with a wide gap for acting as sensitizers due to high mobility charge carriers and stability [39–50]. The limitations of the n-type semiconductor like leaching, bad response toward visible light, thermal decomposition, high rate of recombination of electron, and hole can be overcome by combining p-type CPs with an n-type semiconductor because CPs usually behaves as p-type semiconductors [51, 52].

TiO_2-based polyaniline (PANI) photocatalysts

The outstanding electrical and optoelectronic properties make the study of the conducting polymers at an extensive level [47, 53–58]. Hybrids of several conducting polymers have been designed to obtain required properties that hold the applications in, corrosion protective coatings, catalysis, and numerous others [59, 60]. Among all, Polyaniline (PANI) is considered to be most comprehensively studied conducting polymer since the last 20 years [61]. PANI is cheaper and has distinctive photoelectric, electrical, and optical properties in comparison with other conducting polymers [62]. The repeating units of PANI consist of two moieties in different weights, i.e., reduced (benzenoid) and oxidized (quinoid) state which is its essential feature [63]. New molecular structures with a variety of properties have been obtained by doping PANI on considering the above element [64–66]. Due to its outstanding environmental stability and mechanical flexibility, it has been considered to be p-type material. Anticorrosion coatings, lightweight battery electrodes, sensors, light-emitting diodes, solar cells, photovoltaic

devices, and electromagnetic shielding devices are the various fields in which it has potential applications [67–72]. Having all these applications of PANI, a very small amount of work has been done to degrade organic pollutants by modifying TiO_2 using PANI.

In the present review, PANI–TiO_2 composites have been discussed with its preparation by '*in situ*' chemical oxidative polymerization of aniline to prepare a series of polyaniline–TiO_2 (PANI–TiO_2) nanocomposite powders with dissimilar PANI–TiO_2 ratios. The photocatalytic degradation of various organic pollutants like rhodamine B, malachite green, reactive red 45, methyl orange and methylene blue are used to evaluate the photocatalytic activity of the catalyst under ultraviolet light. PANI–TiO_2nanocomposite catalysts are utilized for cleaning contaminated water because it has higher photocatalytic activity in comparison with pure TiO_2.

Methods used for the synthesis of PANI/TiO_2 nanocomposites

The synthesis of PANI/TiO_2 nanocomposites was carried out by some methods.

In situ polymerization

In situ polymerization is a very effective method of synthesis of polymer nanocomposites which occurs "in the polymerization mixture". It involves the blending of nanomaterial in a solution mixture containing a neat monomer, followed by polymerization. In this method, the covalent linkage between the nanomaterial and matrix occurs. Several research articles have been published on PANI/TiO_2 in situ polymerization over the last few years [73–76]. Template-free synthesis is the preparation of nanocomposites without using any templates or adduct and there is no need to separate product after synthesis. Many researchers used this method to fabricate PANI/TiO_2 nanocomposites as it an easy method to direct synthesize nanocomposites without any hurdle [77]. Zhang and his coworkers prepared powdered samples of PANI/TiO_2 nanocomposites via varying molar ratios of PANI and nanocrystalline TiO_2 in 1.0 N HCl solution with the help of APS [$(NH_4)_2S_2O_8$)] as an oxidant for highly enhanced photodegradation [78]. Sui et al. [79] have also synthesized PANI/TiO_2 nanocomposites by mixing solutions of aniline monomer and TiO_2 in CTAB/hexanol solution and oxidation was carried out by adding a solution of APS in this solution. These solutions were mixed under vigorously stirring for obtaining PANI/TiO_2 nanocomposites. The same procedure for the synthesis of nanocomposites was adopted by Ti et al. [80] for NH_3 (ammonia) sensing application. In some synthesis, *p*TSA (*p*-toluenesulfonic acid) solution was adopted as a reaction medium [81] and some other researchers also adopted the same process with various oxidants and reaction medium to yield PANI/TiO_2 nanocomposites for various applications [82–85].

Template synthesis

Various nanocomposites of PANI/TiO_2 were synthesized by using some templates such as anodized surfactants [86], micelles [87], alumina [88], etc., but due to

addition of any template, some post-synthetic treatments are must for the removal of these templates to gain the desired nanocomposites. In this regard, PANI/TiO_2 nanocomposites were prepared by adding an aniline monomer in a phosphate buffer solution containing prepared TiO_2 nanoparticles with constant stirring as well as ultrasonic action was added to reduce aggregation. In this process, SPS was added during stirring and HRP was added for enzymatic synthesis as well as diluted H_2O_2 was used to start polymerization. In this technique, nanocomposites remain in the form of powder [89]. Nabid and his labmates prepared PANI/TiO_2 nanocomposites by using SDS as a template for controlling the shape and size of these nanocomposites for better results and application [90].

Solgel synthesis

Solgel methods can be applied to alter or modify the properties of nanocrystalline. In the preparation process of PANI/TiO_2 nanocomposites via the solgel method, firstly TiO_2 sols were synthesized by maintaining a water-to-titanium isopropoxide ratio of 4 and 0.0016 mol of aniline monomer was added in this sol and reaction was carried out for 2 h, after that 0.0015 mol APS in HCl solution was added dropwise as an oxidant to get the dark green colored PANI/TiO_2 nanocomposites [91]. Pawar and his labmates synthesized polyaniline (PANI) by chemical oxidative polymerization of aniline monomer in which ammonium peroxidisulphate was used as an oxidant and the reaction was carried out in the presence of hydrochloric acid as a catalyst. Nanocrystalline TiO_2 was synthesized by the solgel technique and its nanocomposites with PANI were prepared by stirring of TiO_2 in various molar ratios in undoped PANI solution and after that, thin films were fabricated at 3000 rpm for 40 s by spin coating method [92].

By mixing of polymer and nanoparticles

In this method, the direct mixing of PANI with TiO_2 nanoparticles occurs. 20 ml of an aqueous solution of PANI was taken to continue stirring up to 8 h via ultrasonication to get complete dispersion of PANI in water. Afterthought, 0.2 g of TiO_2 nanoparticles was added in the above solution to get a stable and uniform solution. After complete reaction, the solution was dried at 50 °C and powdered samples of PANI/TiO_2 were collected for enhanced photocatalytic degradation of Bisphenol A [93].

Gu and his coworkers reported the formation mechanism of two incorporating methods of PANI/TiO_2 composites as effective visible photocatalysts. In conventional incorporating style, TiO_2 nanoparticles having high surface energy were easy to prepare huge aggregates of R phase throughout the synthesis. Then during the polymerization of aniline, PANI covered the surface of TiO_2 aggregates after the addition of oxidant (Fig. 2a). On the other hand, TiO_2 grains were deposited on the surface of PANI nanofiber to synthesize PANI/TiO_2 composites (Fig. 2b) [94].

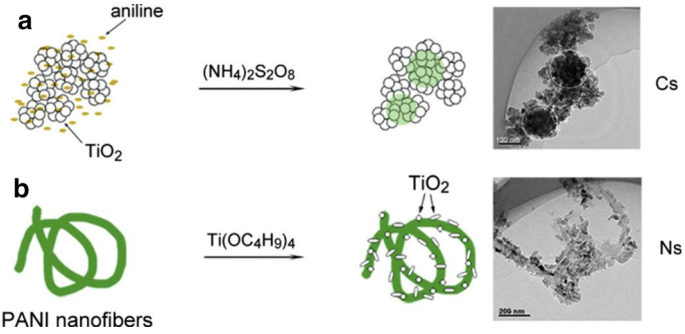

Fig. 2 Synthesis mechanisms of PANI/TiO_2 composites in two incorporating styles: **a** conventional incorporating style and **b** novel incorporating style. Reproduced from Journal of Molecular Catalysis A: Chemical, vol. 357, pp. 19–25 Liuan Gu, Jingyu Wang, Rong Qi, Xiaoyu Wang, Ping Xu, and Xijiang Han, A novel incorporating the style of polyaniline/TiO_2 composites as effective visible photocatalysts, © 2012, with permission from Elsevier

Synthesis and characterization of various PANI–TiO_2 photocatalysts for dye degradation

PANI has been utilized for synthesizing copolymers and composites for advancing their processability [95]. PANI is appropriate for synthesizing PANI–TiO_2 nanocomposites due to a 2.8 eV bandgap of PANI [96–99]. PANI/TiO_2 nanocomposites were synthesized using the in situ oxidative polymerization technique by using a micellar solution of DBSA (dodecylbenzenesulfonicacid) as surfactant as well as the dopant. These nanocomposites were characterized by FTIR, XRD, SEM, TGA, etc., which unveiled decreased bandgap of nanocomposites as compared to pristine nano-TiO_2, while optical responsivity showed vice versa behavior under visible light. Therefore, these were found highly useful in photo-oxidative acrylic pseudo-paints for removal of benzene under UV/VIS lights [97]. Zhu et al. [98] has also prepared PANI/TiO_2 nanocomposites via a one-step hydrothermal process. The characterization of these was done via transmission electron microscopy (TEM), scanning electron microscopy (SEM) and X-ray diffraction (XRD) for investigation of its structure and morphology. These uniform PANI/TiO_2 nanocomposite-based sensors displayed excellent sensitivity (5.4 to 100 ppm), selectivity, long-term stability, repeatability, a good linear relationship, and a low detection limit (0.5 ppm) to sense ammonia at room temperature (20 ± 5 °C). The main reason for the outstanding sensing of ammonia was the creation of the p-n heterostructure in the PANI/TiO_2 nanocomposites. Some researchers also synthesized nanocomposites via using the same process and XRD studies suggested highly crystalline structure of the same, as well as FE-SEM studies, suggested porous structure of nanocomposites and HR-TEM micrographs revealed the irregular shape of TiO_2 nanoparticle sand size was found about 17 nm, as well as TiO_2 nanoparticles, were entrenched within PANI backbone which was an advantage over neat TiO_2 to avoid the absorption of vapors in nanoparticles. The presence of chemical bonding between TiO_2 nanoparticles and PANI chains was confirmed by FTIR spectra [100]. Wang et al. [101] synthesized neat PANI, TiO_2

and PANI/TiO_2 nanocomposites having the size of 80–90 n for nanocomposites, and TiO_2 nanoparticles surface was found covered with PANI films in TEM micrographs of nanocomposites, Fig. 3(i), and hence good electronic contact between PANI and TiO_2 was claimed. In XRD patterns too, there is a lot of difference that could be seen in nanocomposites formation as in case of PANI/TiO_2 degree of crystallinity was decreased, Fig. 3(ii) and diffraction peaks disappeared suggesting an interaction between PANI and TiO_2. These nanocomposites were able to degrade Methylene blue under the irradiation of natural light more efficiently compared to neat TiO_2.

These nanocomposites have been synthesized by Wang and Min [101] for the degradation of methylene blue dye. The average size varying from 80 to 90 nm is obtained by the morphology of PANI-coated TiO_2. The discoloration efficiency PANI/TiO_2 w 80% which was great as compared to neat TiO_2 nanoparticles (NPs) having 34% only, upon 90 min irradiation of UV–Vis light. Numerous photocatalytic runs lasting for 90 min has been made by TiO_2 and TiO_2/PANI to examine the reusability. PANI/TiO_2 has been prepared by Wang et al. [102] by using the method of one-pot chemical oxidative polymerization. They prepared these nanocomposites by using titanium isopropoxide for obtaining TiO_2 and further adding aniline monomer with ammonium isopropoxide for gaining PANI–TiO_2 nanocomposites in powder form. The characterization results revealed the photocatalytic activity of PANI/TiO_2 was about 55% for methylene blue after 4 runs. They also reported the synthesis of PANI-sensitized TiO_2 nanocomposite with varying molar ratios of PANI and TiO_2 by mixing THF (tetrahydrofuran) solution of CSA (camphor sulfonic acid) doped PANI and TiO_2 nanoparticle suspension in ethanol [103]. The photocatalytic activity of composite has been improved by extending the light response of TiO_2 to visible light. When the mass ratio PANI: TiO_2 varies from 1:400 to 1:700 and the optimum sensitized effect was at the mass ratio of 1:500 then methylene dye is degraded more effectively on PANI–TiO_2 as compared to bare TiO_2. The rate constant for methylene dye by PANI/TiO_2 is found to be 1.57 times greater as compared to bare TiO_2. Good photocatalytic stability under visible light has been shown by

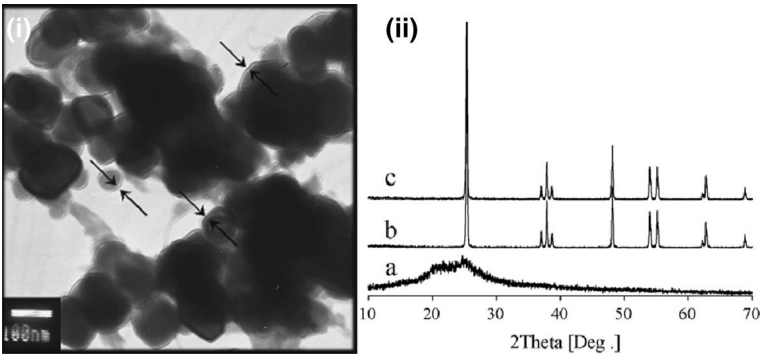

Fig. 3 **i** TEM image of PANI/TiO_2 nanocomposite **ii** XRD patterns of (a) PANI, (b) TiO_2 and (c) PANI/TiO_2 nanocomposites. Reproduced from Chinese Chemical Letters, vol. 18, pp. 1273-1277, Wang, Fang, and Shi Xiong Min. "TiO_2/polyaniline composites: an efficient photocatalyst for the degradation of methylene blue under natural light." © 2007, with permission from Elsevier

PANI/TiO_2 composites after 5 runs. PANI/TiO_2 nanocomposites have been fabricated and used by Salem et al. [104] for the degradation of Quinoline yellow and Allura red, and it has been observed to follow first-order kinetics. On raising the concentration of persulfate and aniline monomer, the photocatalytic activity was also raised. $H_2SO_4 > H_3PO_4 > HCl > HNO_3$ is the order of composites that were prepared in the presence of various acids as the dopant. Figure 4 represents the preparation of PANI/TiO_2 nanocomposites by Olad et al. [105] with 21 nm average crystal size.

Degradation of dyes via PANI–TiO_2 photocatalysts

The photocatalytic degradation of organic pollutants is chiefly done for dyes as dyes such as methylene blue (MB), rhodamine B (RhB), etc., from textile industries and household raise many toxic pollutants and considerable concern in water due to harmful toxic and environmental effects on ecological systems [106–108].

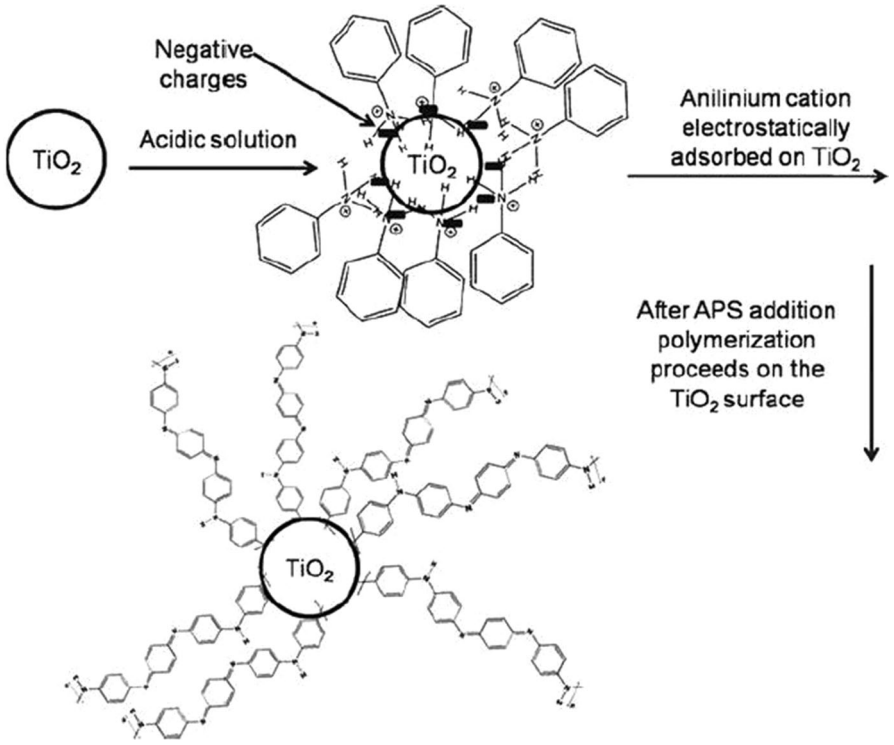

Fig. 4 Formation scheme of PANI/TiO_2 core–shell nanocomposite. Reproduced from Bulletin of Material Science, Vol. 35, pp. 801–809, Ali Olad, Sepideh Behboudi, Ali Akbar Entezami, Preparation, characterization and photocatalytic activity of TiO_2/polyaniline core–shell nanocomposite, © 2012 with permission of Springer

Degradation of various dyes has been studied widely in literature via photocatalysis of PANI–TiO_2 nanocomposites [85, 109–113].

Degradation of methylene blue (MB) by using PANI–TiO_2 Photocatalysts

The photocatalytic degradation of methylene blue dye in sunlight has been investigated by Yu et al. [114] by synthesizing PANI/TiO_2 composite fiber films as a result of electrospinning, calcinations, and in situ polymerization. The polymerization temperature of aniline in the composite and crystal structure of TiO_2 was associated with photocatalytic activity. It has been observed that PANI/TiO_2 composite film was not able to degrade methylene blue in 4 h under photocatalytic action, but it can be degraded by TiO_2 fiber films under photocatalytic action in 3 h. The microstructure of PANI nanowire grown on TiO_2 nano/microfiber with the microstructure of PANI grown on it showed low contrast PANI. The rate of decoloration of methylene dye by utilizing composite film was found to be equal to pristine TiO_2 film on 4-h irradiation. The rate of decoloration of methylene blue using PANI/TiO_2 is decreased as compared to pristine TiO_2 film when the time of irradiation increased from 4 h. It has been observed from the numerous photocatalytic runs that methylene blue decolorized completely after 4 runs using TiO_2 film and PANI/$TiO_2$was able to degrade only 15% methylene blue after 4 runs in 2 h. During the photocatalytic process, there was a gradual degradation due to the poorer reusability of PANI/TiO_2composite fiber film compared to the TiO_2 film. Ahmad and Mondal [115] utilized PANI/TiO_2 nanocomposites for the effective degradation of Methylene blue. They also represented a possible mechanism for dye degradation, Fig. 5. When PANI/TiO_2 surface was illuminated with light energy, valence band holes and conduction band electrons generated due to greater energy given on the PANI/TiO_2 surface than the bandgap of the nanocomposite. The photogenerated holes can either react with water of hydroxide to create hydroxyl radicals or can oxidize any organic molecule and photogenerated electrons can either do the reaction with electron acceptors to form superoxide or can reduce the dye. The degradation of methylene blue dyes can be understood by the following equations in Fig. 5.

The photocatalytic activity of the nanocomposites is developed by the deposition of PANI on TiO_2 NPs. Pristine TiO_2 revealed 89% degradation of dye, while 93% of degradation was observed by the PANI/TiO_2nanocomposite. The enhancement in the specific surface area, large interaction between composite photocatalyst results in a decrease in aggregation in the nanocomposite which is the reason behind the enhancement of photocatalytic degradation of nanocomposite in comparison with pristine TiO_2. Methylene blue and rhodamine B has been degraded by a two-step route given by Wang et al. [94] using PANI/TiO_2 nanocomposites with different PANI to TiO_2 NPs mass ratios. The nanocomposites of PANI to TiO_2: 0.5/100, 0.75/100, 1/100, 2/100, and 5/100 were designated as N0.5, N0.75, N1, N2, and N5, while PANI to TiO_2 at 1/100 had been designated as C1. The average particle size was calculated and found 11.6–12.5 nm. PANI was shown to act as a good photosensitizer for enhancement of light absorption from visible to the near-infrared region, and therefore the visible photocatalytic activity was improved with a scarce decrease in UV photoactivity, shown in Fig. 3 [94]. With increasing the mass of PANI from 0

$$PAni - TiO_2 + h\gamma \xrightarrow{light} PAni - TiO_2(e^-_{CB} + h^+_{VB}) \quad [1]$$

$$PAni - TiO_2(e^-_{CB} + h^+_{VB}) \xrightarrow{light} PAni - TiO_2 + heat \quad [2]$$

$$PAni - TiO_2(h^+_{VB}) + H_2O \rightarrow PAni - TiO_2 + H^+ + OH^{\cdot} \quad [3]$$

$$PAni - TiO_2(h^+_{VB}) + OH^{\cdot} \rightarrow PAni - TiO_2 + OH^{\cdot} \quad [4]$$

$$PAni - TiO_2(e^-_{CB}) + O_2 \rightarrow Pani - TiO_2 + O^{\cdot -}_2 \quad [5]$$

$$O^{\cdot -}_2 + H^+ \rightarrow HO^{\cdot}_2 \quad [6]$$

$$MB + OH^{\cdot} \rightarrow \text{Degradation products} \quad [7]$$

$$MB + h^+_{VB} \rightarrow \text{Oxidation products} \quad [8]$$

$$MB + e^-_{CB} \rightarrow \text{Reduction products} \quad [9]$$

Fig. 5 Photodegradation of Methylene blue dye by using PANI/TiO_2 nanocomposites. Reproduced from Journal of dispersion science and technology, Vol. 33, pp. 380–386, Ahmad, Rais, and Pijush Kanti Mondal. "Adsorption and photodegradation of methylene blue by using PAni/TiO_2 nanocomposite." © 2012 with permission of Taylor & Francis

to 1/100, photoactivity of composites was gradually enhanced. The rate of degradation was still high on using PANI as compared to TiO_2.

Nanocomposites of PANI/TiO_2 have been synthesized by Radoičić et al. [116] utilizing molar ratios 50, 100, and 150 of TiO_2/aniline by oxidative polymerization. 50, 100, and 150 were the mole ratios for [TiO_2]/[ANI] which has been used to prepare nanocomposites of PANI/TiO_2 and TP-50, TP-100, and TP-150 were used for the mole ratio of [APS]/[ANI]¼ (1.25). The photodegradation reaction of methylene blue and rhodamine B in a suspension has been used to determine the potential applicability of prepared PANI/TiO_2 nanocomposites as a photocatalyst. It has been reported that all nanocomposites were able to degrade methylene blue and rhodamine B faster as compared to pristine TiO_2. The nanocomposites TP-50, P/T-100, and P/T-150 were able to remove 85% of rhodamine B and 20% of methylene blue from the solution of dye at the exposure of 360 min, while 17% of rhodamine B and 5.5% of methylene blue was removed from the same solution using nanoparticles of pristine TiO_2 at the same time of exposure. TP-50/TP-100 has been used to achieve excellent photocatalytic activity. It has been observed that only 60% of methylene blue was degraded within 360 min and rhodamine B completely degraded after the same time. The interaction of hydroxyl groups of the TiO_2 nanoparticle with carboxyl groups of rhodamine B dyes was responsible for the increase in PANI content in the nanocomposite and hence the photocatalytic activity of PANI/TiO_2nanocomposites increases in the process of rhodamine B degradation. If the PANI-emeraldine salt formed was chief, then there was a repulsion between the cationic groups of dyes and the positively charged chains of PANI-emeraldine and hence it was

responsible for the hindrance in the repulsion of rhodamine B dyes with the surface of TiO_2 nanoparticles. The optimal photocatalytic activity of the TP-100 nanocomposite sample had been argued by the protonation of PANI-EB form with the carboxyl group of RB, which revealed increased electrostatic interaction between PANI chains and dye molecules and consequently to better photocatalytic activity. Zhi et al. [117] have been synthesized homogenous composite of PANI/TiO_2 utilizing peroxy-titanium complex which acts as a TiO_2 precursor and the oxidant by emulsion polymerization technique. Poly(ethyleneterephthalate) (PET) film as a substrate was used for photocatalytic activities of nanocomposites of PANI/TiO_2 for studying the degradation of methylene blue dyes. When the molar ratio of aniline to Ti was taken 1/1 in the PANI/TiO_2 nanocomposite, excellent conductivity and photocatalysis are observed in Fig. 6.

The electrons generated from PANI have been transferred to the conduction band of TiO_2 and holes that have been transferred from the valence band of TiO_2 are facilitated due to the similarity between the highest occupied molecular orbital (HOMO) of TiO_2 and LUMO of PANI which is responsible for the increased catalytic behavior. Photocatalytic performance has also been increased due to enhancement in the adsorption capacity of organic pollutants which is caused due to intermolecular interaction between PANI and dye molecules over nanocomposites.

Wang et al. [103] synthesized PANI doped with camphor sulfonic acid (CSA)/TiO_2 nanocomposites via dispersion polymerization method for photocatalytic experiments by using different initial mass ratios of PANI to TiO_2. 1:200, 1:300, 1:400, 1:500, 1:600 and 1:700. These nanocomposites were designated as PANI/

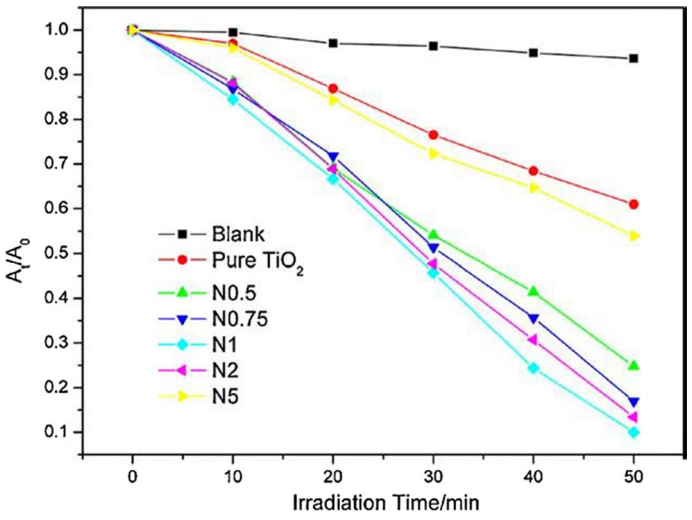

Fig. 6 The time courses of RB degradation ratefor TiO_2 and Ns under visible light irradiation with different mass ratios of PANI to TiO_2 at 0.5:100, 0.75:100, 1:100, 2:100, and 5:100. Note: RB, rhodamine B; PANI, polyaniline. Reproduced from Journal of Molecular Catalysis A: Chemical, vol. 357, pp. 19-25 Liuan Gu, Jingyu Wang, Rong Qi, Xiaoyu Wang, Ping Xu, and Xijiang Han, A novel incorporating the style of polyaniline/TiO_2 composites as effective visible photocatalysts, © 2012, with permission from Elsevier

TiO_2 (1:200), PANI/TiO_2 (1:300), PANI/TiO_2 (1:400), PANI/TiO_2 (1:500), PANI/TiO_2 (1:600) and PANI/TiO_2 (1:700).

The adsorption capacities were increased in the dark by the introduction of PANI to the nanocomposites. The adsorption capacity of the composite of PANI/TiO_2 firstly increased and then started decreasing by decreasing the content of PANI. 1:500 mass ratio of PANI to TiO_2 represents the highest capacity of adsorption of the composite of PANI/TiO_2. The change in the structure of the surface results in the variation in the capacity of adsorption of the composite of PANI/TiO_2 with the change in the PANI to the TiO_2 mass ratio [118]. It has been observed from the experiment that the self-photolysis of methylene blue is slow in the absence of photocatalyst and after the irradiation of visible light for 120 min; the efficiency of degradation is lower than 34%. In photocatalysis, firstly there was an increase in the photocatalytic activity but then it starts to decrease with the decrement of PANI to TiO_2 mass ratio from 1:200 to 1:700. Composites with PANI to TiO_2 mass ratios from 1:400 to 1:700 exhibit clear synergetic effect between PANI and TiO_2, PANI to TiO_2 mass ratio from 1:500 exhibit optimum of the sensitized effect. The photocatalytic activity of composite photocatalyst was lower due to occupation of active sites of TiO_2 by a large amount of PANI which results in rapid degradation of methylene blue dyes as it is unable to reach the active sites of the TiO_2 nanoparticles and hence under visible light irradiation, more electron holes pair generated with time. In UV–visible spectra, fast dye degradation of methylene blue at adsorption peak 664 nm was observed. During the irradiation, the shift of peak was from 664 to 630 nm in the absorption maximum wavelength. The N-demethylated derivatives of methylene blue are characterized by blue-shifted absorption. The absorption spectra of the mixture of N-demethylated analogs of methylene blue in the visible region were broadened. Zhang et al. [119] also observed the broadening and the blue shifts of the absorption bands in aqueous semiconductor TiO_2 dispersions during photo-oxidative degradation of methylene blue under irradiation with UV light. A simple method was employed for the synthesis of PANI-sensitized TiO_2 composite photocatalysts. The photoresponse revealed that the photocatalytic efficiency of the nanoparticles (NPs) of TiO_2 was extended by the use of PANI.

The degradation of methylene blue in an aqueous solution under visible light has been carried out to evaluate the photocatalytic activity of the resulting composite photocatalysts. PANI-sensitized TiO_2 composite photocatalysts with certain mass ratios of PANI to TiO_2 showed higher photocatalytic activity than bare TiO_2 under visible light; PANI/TiO_2 (1:500) achieved the best performance. This can be attributed to the sensitized effect of PANI and the charge transfer from the photoexcited sensitizer to TiO_2. Also, the composite photocatalysts have good photocatalytic stability and can be reused five times with the only gradual loss of activity. Thus, the PANI/TiO_2 nanocomposites were efficient photocatalytic materials for degrading contaminated colored wastewater for reuse in textile industries under mild conditions [120].

Degradation of methyl orange (MeO) and orange II

Photocatalytic degradation of MeO and orange II has been investigated by preparing PANI–TiO_2 composite nanotubes by Cheng et al. [84] using the assembly method. PANI/TiO_2 composite and PANI nanotubes showed a degradation rate of 98.1 and 95.6% for MeO and both have high photocatalytic activity. The decolorization efficiency was 98.6% as compared to 76.7% for PANI nanotubes when PANI/TiO_2 composite nanotubes were used as the catalyst. Naphthalenesulfonic acid (a-NSA) has been used by Cheng et al. [84] as the dopant for the synthesis of PANI and PANI/TiO_2 nanocomposite by the self-assembly to carry out the degradation of MeO and orange II. PANI/TiO_2 composite nanotubes with size 200–400 nm were used for the photodegradation of MeO and orange II under UV irradiation. 91.3% was the rate of decolorization of orange II for nanocomposite and 94.2% for PANI nanotubes. Pseudo-first-order reaction kinetics has been followed by photocatalytic degradation. Due to the low surface area, the TiO_2 rate constant was greater than composite nanotube and PANI, i.e., 0.023 and 0.021 min^{-1}. For the photocatalytic investigation of MeO, a similar process has been executed. Decolorization of MeO for composite nanoparticle was found to 69.5% and 97.2% for PANI nanotubes which were utilized as a catalyst. The rate constant for composite nanotubes and normal PANI were 0.027 and 0.012 min^{-1}. Pseudo-first-order kinetics was followed in the photocatalytic degradation. Transfer of photo-induced radical energy from PANI to TiO_2 was responsible for the slower degradation rate of MeO as compared to orange II. The photocatalytic activity of nanocomposite was investigated against methylene blue by Jeong et al. [121] by formulating a one-dimensional morphology of nanocomposite tubes utilizing PANI/TiO_2 hybrid. After 300 min of exposure, the degradation efficiency of methylene blue was 11 % for PANI nanotubes, 39% for TiO_2 NPs, and 85% for nanocomposites. The efficiencies for methylene blue decomposition were recorded 58, 71, 77 and 65% PANI, TiO_2, PANI–TiO_2–S, and nanocomposite. Nanostructures of PANI and the joint effect of PANI and TiO_2 constituent in the hybrid were responsible for the origination of PANI–TiO_2-S with the highest efficiency. Electronic transition and the intersystem crossing were responsible for the production of singlet and triplet species which explained the degradation of methylene blue. Advance oxidation species generated by TiO_2, PANI, and their hybrid catalyst were able to degrade the methylene blue [122]. In the mechanism of photosensitization, it has been explained that excited electron of PANI (e^- CB) was injected into CB of TiO_2, which then reached the surface and upon reaction with O_2, generated O_2^- species, while h^+ in VB reacted with OH group that generated OH^o. TiO_2 facilitated the charge separation in PANI, whereas PANI-sensitized TiO_2 in the visible region as shown in Fig. 6.

For visible-light photocatalytic activity toward degradation of MeO, *Lin et al.* [123] synthesized flexible nanofiber membranes of TiO_2/SiO_2. The amount of loading of PANI was found 1.0%, 2.3%, 2.6%, and 5.1% on the TiO_2/SiO_2 nanofiber membrane for P/TS-0.5, P/TS-1, P/TS-2, and P/TS-4 samples. P/TS-1 > P/TS-0.5 > P/TS-2 > P/TS-4 > P/S > TS > TiO_2 > blank was the order for the efficiency of photocatalytic degradation of MeO under visible light. P/TS-1 nanofiber membrane had shown excellent photocatalytic activity under visible light and MeO was

degraded by 87% in one and a half hours (Figs. 7, 8). The active sites of the photocatalysts have been blocked by the presence of residual organic dyes in the nanofibers which were responsible for the decrease in the photocatalytic activity shown in Fig. 9. The degradation of methyl orange by PANI/TiO_2 is also shown in Fig. 9.

Hydrothermal process and low-temperature calcinations treatment methods were used by Liu and coworkers [124] for the synthesis of PANI/TiO_2 nanocomposites. The photocatalytic activity of nanocomposite of PANI/TiO_2 was higher as compared to bare and nitrogen-doped TiO_2. The good photocatalytic activity has been

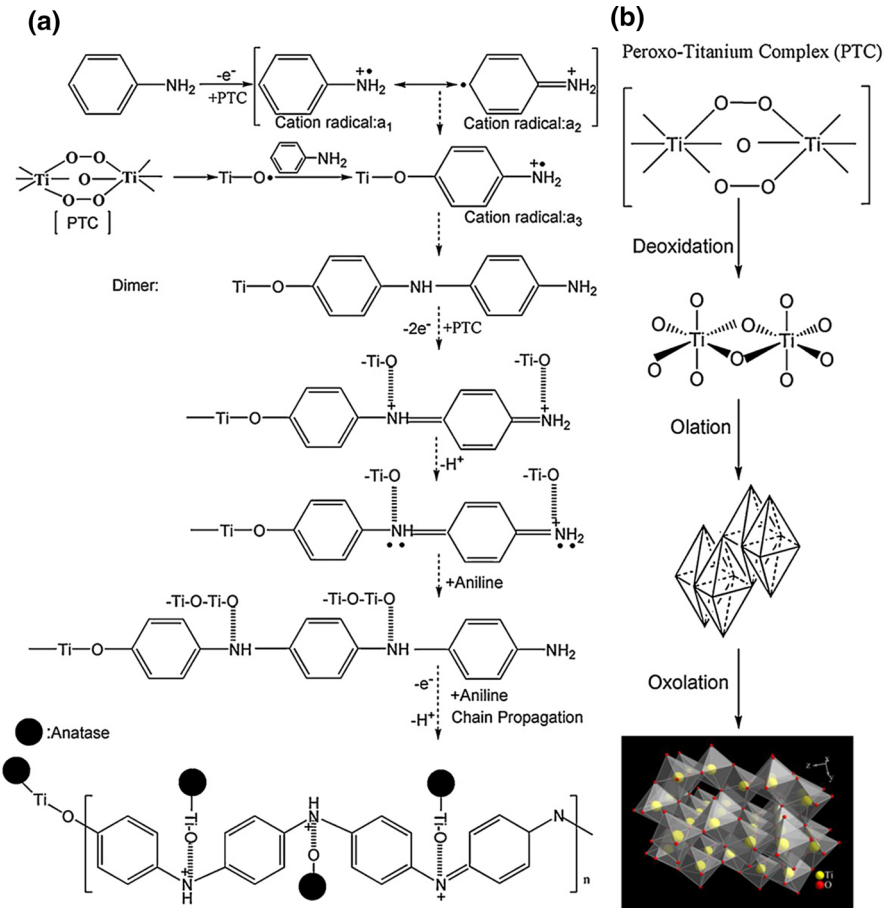

Fig. 7 A representation of the reaction mechanism of PANI/TiO_2 nanocomposites: **a** the oxidative polymerization of aniline initiated by PTC, **b** the formation of anatase-type TiO_2 from PTC precursor. B **a** Photocatalytic degradation efficiency and conductivity of PANI/TiO_2 nanocomposites with different molar ratios of AN/Ti, **b** Photocatalytic degradation curves of aqueous MB irradiated under UV light (365 nm) over the PANI/TiO_2 nanocomposite, Anatasesol and bulk PANI. Note: PANI, polyaniline; PTC, peroxo-titanium complex; MB, methylene blue. Reproduced from Applied Surface Science, vol. 273, Yuzhen Li, Yuan Yu, Liangzhuan Wu, Jinfang Zhi, Processable polyaniline/titania nanocomposites with good photocatalytic and conductivity properties prepared via peroxo titanium complex catalyzed emulsion polymerization approach, 135–143, © 2013, with permission from Elsevier

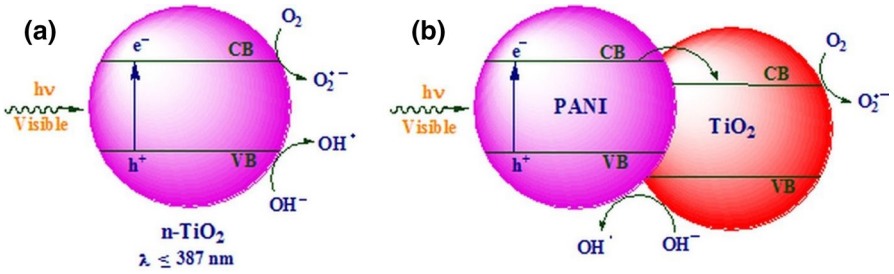

Fig. 8 Schematic of the band excitation and advanced oxidation species formation in **a** TiO_2 and **b** PANI–TiO_2–S hybrid photocatalyst. Reproduced from Polymer-PlasticsTechnology and Engineering, Vol. 54 (17), pp. 1850–1870, Ufana Riaz, Ashraf SM, Jyoti Kashyap, Role of Conducting Polymers in Enhancing TiO_2-based Photocatalytic Dye Degradation: A Short Review, © 2015 with permission of Taylor & Francis

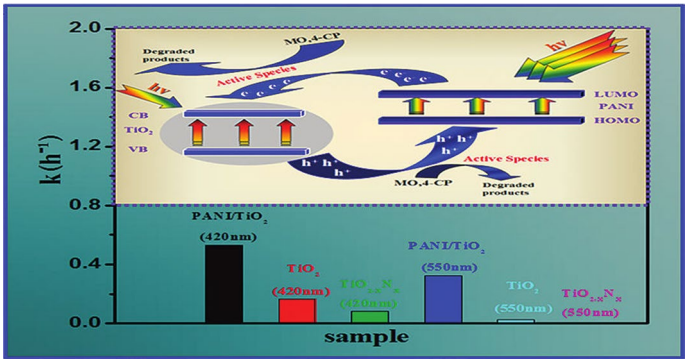

Fig. 9 Mechanism of degradation of Methyl Orange by PANI–TiO_2 photocatalysts. Reproduced with permission from ACS, J. Phys. Chem. C 116, pp 5764–5772, Yangming Lin, Danzhen Li, Junhua Hu, Guangcan Xiao, Jinxiu Wang, Wenjuan Li, and Xianzhi Fu, Highly Efficient Photocatalytic Degradation of Organic Pollutants by PANI-Modified TiO_2 Composite © 2012, with permission of ACS

exhibited by photocatalyst of PANI/TiO_2 under the longer wavelengths of light toward 4-chlorophenol and MeO. The greater mineralization rate of 4-chlorophenol and MeO in comparison with pristine TiO_2 has been exposed by the total organic carbon under visible and UV irradiation, 3.0 at 100 °C, 2.95 at 150 °C, and 2.80 eV at 200 °C were the expected bandgap of the PANI/TiO_2 nanocomposite corresponding to different temperatures. From this, it is clear that nanocomposites revealed narrow bandgap as compared to pristine TiO_2. No activity was exhibited by organic pollutant in absence of photocatalyst and the increase in temperature resulted in an enhancement in photocatalytic activity. Nitrogen-doped TiO_2 was utilized as a reference catalyst. The order for the efficiency of degradation of MeO in visible light was as follows

Blank < P/T-100 °C < TiO_2-100 °C < TiO_2-200 °C < P/T-150 °C < P/T-200 °C. From Fig. 8, it has been observed that the outstanding photocatalytic activity under visible light has been exhibited by nanocomposite of PANI/TiO_2 at 200 °C

for the MeO degradation. The rate of degradation of MeO over PANI/TiO_2 at 200 °C was better than of pure TiO_2 at 200 °C in visible light.

The key point is a wide and strong absorption band of PANI in the visible region makes it easy to excite charge transfer from HOMO to LUMO and then offer an electron to the CB of TiO_2 and itself accept a hole from VB of TiO_2 leading to a restraining of the recombination of the electron–hole pair and finally promoting the migration efficiency of photogenerated electron–hole on the interface. The other factor is the increased absorptivity of pollutants over photocatalyst and consequently affecting the photocatalytic performance. The experiments of TOC also reflect that PANI has a special role in the photocatalytic process.

The photocatalytic activity of the PANI-modified composite of $CoFe_2O_4$–TiO_2 has been studied by Leng et al. [125] toward the degradation of methylene blue under irradiations of UV and visible light (Fig. 10). The photocatalytic activity has been increased due to the synergistic effect between PANI, TiO_2, and $CoFe_2O_4$. The recombination of holes and electrons was blocked as the layer of PANI acts as a barrier between the active shell of TiO_2 and magnetic $CoFe_2O_4$. The pairs of electron and holes have been generated under visible light due to the absorption of photons by PANI and $CoFe_2O_4$. From Fig. 11a, the Type 1 nanocomposites demonstrate that the photo-generated electrons from the lowest unoccupied molecular orbital of PANI were transferred to the conduction band of TiO_2 and after that, it jumps to the conduction band of $CoFe_2O_4$. From Fig. 11b, Type 2 nanocomposite demonstrates that the holes in the valence band of $CoFe_2O_4$ jumps to the valence band of TiO_2 and after that, it has been transferred to HOMO of PANI which results in slow recombination of charge and fast separation of charge.

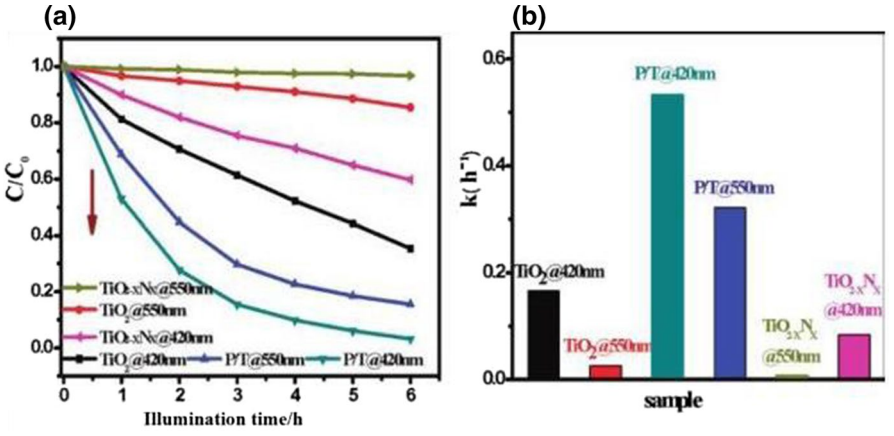

Fig. 10 Process of photocatalytic degradation of MeO, **a** C/Co vs illumination time plot, **b** the comparison of kinetic constants over the P/T-200 °C, TiO_2-200 °C, and TiO_2-xNx under visible light with different wavelengths (420 nm < k < 800 nm, 550 nm < k < 800 nm) Reproduced with permission from ACS, *J. Phys. Chem.* C 116, pp 5764–5772, Yangming Lin, Danzhen Li, Junhua Hu, Guangcan Xiao, Jinxiu Wang, Wenjuan Li, and Xianzhi Fu, Highly Efficient Photocatalytic Degradation of Organic Pollutants by PANI-Modified TiO2 Composite © 2012, with permission of ACS

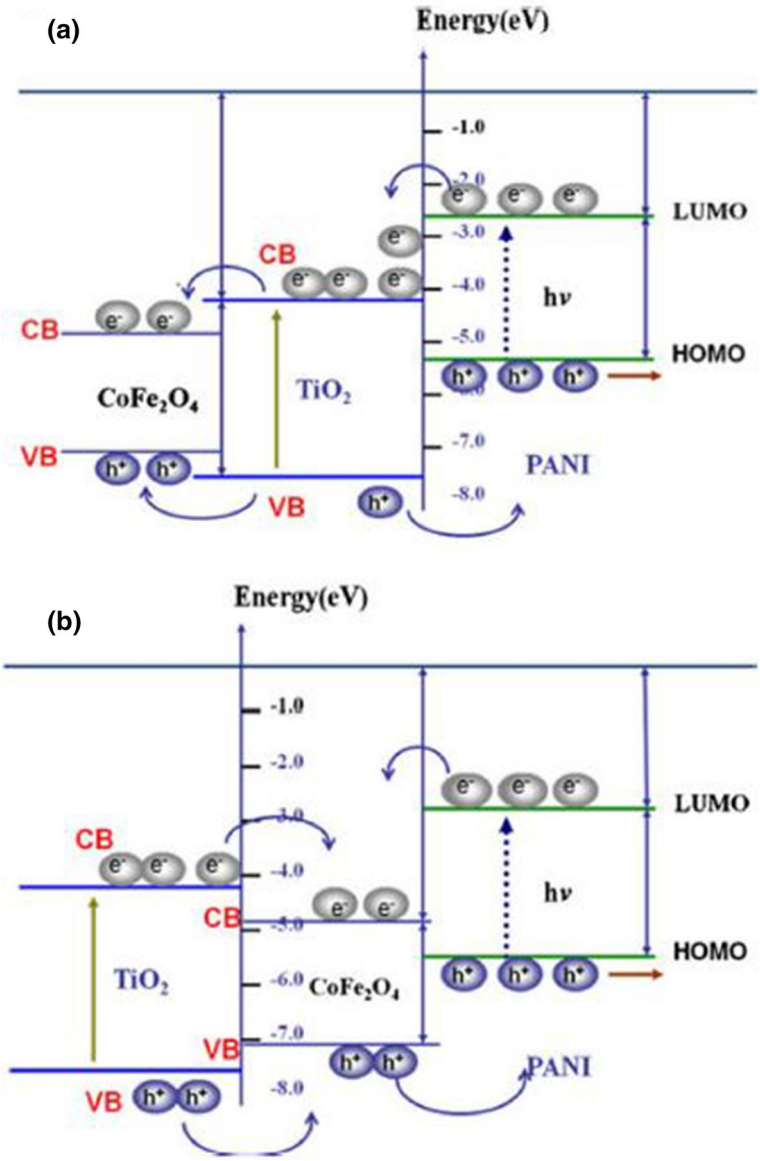

Fig. 11 Possible charge carrier transfer mechanism in the $CoFe_2O_4$–TiO_2- nanocomposites (PCT) system under UV light irradiation **a** the $CoFe_2O_4$ is encapsulated in the TiO_2 matrix and **b** the iron oxide phase is fixed on the surface of TiO_2. Reproduced from Polymer-PlasticsTechnology and Engineering, Vol. 54 (17), pp. 1850–1870, Ufana Riaz, Ashraf SM, Jyoti Kashyap, Role of Conducting Polymers in Enhancing TiO_2-based Photocatalytic Dye Degradation: A Short Review, © 2015 with permission of Taylor & Francis

The thermal method of degradation has been used by Zarrin and Heshmatpour [126] for the preparation of nanocomposites of TiO_2/Nb_2O_5 and TiO_2/Nb_2O_5/RGO. Likewise, the hydrothermal method and in situ chemical oxidative polymerization method was used for the synthesis of TiO_2/Nb_2O_5/PANI nanocomposite.

At the pH = 9 and pH = 5, excellent photocatalytic activities have been obtained for MB and MeO. Zero-point charges are near to pH = 6.9 for TiO_2 photocatalyst and its surface charge is equivalent to zero. The surface of the catalyst has a negative charge in the basic conditions and positive charge in the acidic medium. The reaction of –OH ions with the positive pores of the catalyst surface is responsible for the generation of hydroxyl radicals and has an important function in the decolorization process [127]. The concentration of hydroxyl radicals decreases as a result of a decrease in –OH ions due to the presence of H^+ ions in the acidic medium. The efficiency of decolorization decreased in some conditions. The greater number of hydroxide ions in the reaction solution leads to the creation of more hydroxyl radicals in the basic medium. From the previous observation, it is observed that the methylene blue has a cationic appearance in solution. Methylene blue can be easily adsorbed onto the photocatalyst because of the significant negative charge on the surface of the photocatalyst [128].

The adsorption will be retained by the acidic solution. Many primary oxidants are produced due to the photo-degradation of methylene blue which in turn results in the production of hydroxyl radicals due to oxidation of adsorbed water. But the methyl orange exhibit anionic form in the solution. The rate of photo-degradation in the present experimental situation depends upon the effect of pH. The rate of photo-degradation was higher in the case of acidic situations as compared to the basic situations. For the photo-degradation of methyl orange, similar results for pH effect were obtained [129]. High photocatalytic activity in the acidic medium was due to the absorption of negatively charged methyl orange on the positive surface of the photocatalyst which results in the decolorization reaction. The rate of photo-degradation in the basic condition decreases due to the coulombic repulsion between dye anion and the photocatalyst surface which was negatively charged and hence there is a decrease in the absorption of methyl orange photocatalyst surface. The photodegradation of methylene blue is superior to methyl orange. As RGO supply negatively charged surface, hence the methylene blue can be adsorbed on the surface of the catalyst. The large molecular size of the methyl orange as compared to methylene blue results in its lesser degradation. The hydroxyl radicals formed on the interface of nanocomposite and the adsorption of dye onto the surface of the photocatalyst are the factors on which the photodegradation of the dye depends. The two dyes struggle for the adsorption at the photocatalyst's surface because the chemical and physical properties of different dyes are different [130, 131]. The photocatalytic activity of TiO_2/Nb_2O_5/RGO is found to be highest in comparison with pure TiO_2, TiO_2/Nb_2O_5, and TiO_2/Nb_2O_5/PANI for the removal of methylene blue and methyl orange. The photocatalytic activity of TiO_2 NPs increases due to the existence of both RGO and Nb_2O_5.

The obtained results have been indicated that TiO_2/Nb_2O_5/RGO has the highest photocatalytic activity in the removal of MB and MO dyes under visible light with the TiO_2/Nb_2O_5/PANI, TiO_2/Nb_2O_5, and pure TiO_2 samples. Therefore, due to the

presence of both Nb_2O_5 (with the separation efficiency for photo-generated electron–hole pairs) and RGO (with high electrical conductivity and adsorption ability), this modification has been considered to be a simple and appropriate method for enhancing the photocatalytic activity of TiO_2 nanoparticles. The TiO_2/Nb_2O_5/RGO also exhibits higher photocatalytic efficiency about the TiO_2/Nb_2O_5/RGO, $TiO_2/Nb_2O_5$and pure TiO_2 nanoparticles. It can be related to various reasons such as high electrical conductivity, low degree of aggregation, the smallness of particle size, and large specific area [126].

Degradation of malachite green (MG)

Different methods have been used for the preparation of nanocomposites of PANI/TiO_2 for degradation of malachite green. Samarah and Kumar [132] synthesized nanocomposites of PANI/TiO_2 by adding DBSA to distilled water via stirring and adding TiO_2 to the above solution. After that, aniline was added to reaction mixture to yield PANI-TiO_2 nanocomposites. The photocatalytic activity of pure TiO_2 NPs is less than the PANI–TiO_2 nanocomposites, for malachite green, a similar degradation condition is used for bulk PANI and PANI NPs. The oxidative property of the TiO_2 NPs increases due to the transfer of an electron from TiO_2 to PANI and hence increases the photocatalytic activity of nanocomposites. Electron–hole pair is generated by PANI–TiO_2 nanocomposite by absorbing energy related to the band-gap. The adsorption of energy in the form of heat has been released nonradiative due to the recombination of hole and electron. MGH^- is the reduced form obtained by the combination of a proton and two electrons with cationic dye MG^+. For the photocatalytic degradation of MG (Malachite green), this step is the rate-determining step. CO_2 and NH_4 were the end products formed by the degradation of *the leuco* form of the dye. The oxidative efficiency of the TiO_2 NPs increases by the transfer of the electron from the CB of TiO_2 to the PANI empty states and hence makes the (Valance Band) VB of TiO_2 stable. Strong oxidative–reductive states of the oxide NPs have been formed due to the formation of VB hole and CB electron by absorption of energy by PANI and then there is a transfer of energy is likely to NPs. The charge separation has been achieved by attacking PANI particles on the TiO_2 surface and electron generated can be taken away from the TiO_2 surface. Due to this more effective photocatalyst has been achieved. It has been observed that due to the transfer of charge between two semiconductors, increased separation of the photogenerated holes and electrons [133]. The CB of PANI acts as a sink for the photogenerated electrons as the TiO_2 band is higher than that of PANI's CB. PANI consisting of photogenerated holes was trapped in TiO_2 particles because photogenerated electrons and holes move in a different direction. The full conjugated chromophore structure of the malachite green dye has been degraded by the photodegradation mechanism due to the decrease in the characteristic absorption band of malachite dye and no hypsochromatic shift appears [134]. Photoluminescence spectroscopy has been utilized for the confirmation of higher photocatalytic activity for the oxidation of malachite dye on the PANI–TiO_2 nanocomposite. Also, there was a decrease in the rate of recombination of excited charge carriers due to the transfer of electrons from TiO_2 to PANI [135]. Saramah and his labmates studied degradation

of Malachite green (MG) by UV illumination using TiO2, PANI and PANI/TiO_2 nanocomposites. Radiation of energy was absorbed by PANI/TiO2 nanocomposites equivalent to its bandgap to generate electron and holes pair. Afterthought, holes, and electrons release energy in the form of heat by recombining nonradiative. The rate-determining step of this mechanism is a malachite green dye in the form of a cation recombining with a proton and two electrons to create a reduced form of malachite green. Finally, the reduced form of dye degrades to the final product, i.e., NH_4 and CO_2 [132].

Photocatalytic degradation activities of MG have been studied using PANI–TiO_2 nanocomposite. The rate of degradation of the dye was faster in the presence of PANI–TiO_2 nanocomposite as compared to that with pure TiO_2. This can be attributed to faster electron–hole separation in PANI–TiO_2 nanocomposite which increases the oxidative properties of TiO_2. Hence, the photo injected PANI–TiO_2 nanocomposite can act as a promising photocatalyst for the degradation of MG in industries and laboratories. Higher photocatalytic activity in the oxidation of MG on PANI–TiO_2 nanocomposite has been confirmed by photoluminescence spectroscopy which suggests that photoinjected electrons were transferred from TiO_2 to PANI, thereby decreasing the recombination rate of excited charge carriers [136].

Degradation of azo reactive red 45 (RR45) dye

Gilja et al. [137] used ammonium persulfate for the oxidation of aniline monomer in the presence of TiO_2 for obtaining nanocomposites. Mole ratio of n(Aniline): n(Ammonium persulfate) was taken 1:0.25 for the polymerization. 10%, 15%, 20%, and 25% were the weight ratio of PANI in the composites. 0.8 g of TiO_2 has been taken in all procedures. 0.10 was the weight ratio of oxidized PANI versus TiO_2 in the case of the composite of 10PANI/TiO_2. Different photocatalyst has been synthesized similarly as a sample of 10PANI/TiO_2 which was as follows:

(a) The stable solution has been obtained by using TiO_2 (0.8 g) and sulfuric acid (0.055 ml) and then sonicated for about 15 min to obtain 50 ml of aqueous solution A.
(b) 0.392 mL of aniline and 0.055 mL of sulfuric acid has been used for the preparation of aqueous solution B (50 ml).
(c) 50 mL aqueous C solution has been prepared using 0.245 g of ammonium persulfate and 0.055 mL of sulfuric acid for the preparation of aqueous solution C (50 ml).

Solution A and solution B have been mixed in a reactor container at a rate of 500 rpm for obtaining a stable suspension of aniline-TiO_2 and stirred for about 15 min. The solution C has been added to the reactor container for the in situ polymerization process then the total reaction mixture of 200 ml has been obtained by adding water. The solution has been stirred at room temperature for a day. A similar procedure to 10PANI/TiO_2 has been employed for the preparation of pure PANI samples but TiO_2 was not added. A dark green product has been obtained by the in situ polymerization

process and then the end product was washed with water. Centrifuged and then dried for a day at 60 °C.

Discoloration monitoring through photocatalysis has been used to find out the degradation of the chromophore group of azo RR45 dye (reactive red) (Scheme 1). Total organic carbon has been determined to investigate the degree of mineralization of RR45 azo dye from nontoxic species [138]. 15PANI/TiO_2 photocatalyst has given better performance and has been used for the degradation of RR45 by which 80% of total organic carbon (TOC) was removed and 35% and 41% TOC has been removed by using TiO_2 and 10PANI/TiO_2. Photocatalysis and efficiency of the catalyst are the conditions on which the degree of degradation of the RR45 dye depends. It has been observed that the 15PANI/TiO_2 catalyst was most effective for the degradation of RR45 azo dye as compared to other catalysts and TiO_2. The decomposition products formed which were harmful are not able to block the catalyst and hence the 15PANI/TiO_2 nanocomposite was successful for the photocatalytic wastewater treatment [139].

The generation of excited electrons and holes by absorbing photons with energy higher than 3.2 eV was suggested by Umar et al. [140]. If the holes from the valence band and electron from the conduction band are jumped to the surface of TiO_2 then only the photocatalytic reaction will take place [141]. The immobile active sites of TiO_2 are partially blocked by the formed intermediates because the process of degradation is not always complete. The active sites of the PANI are partially immune to the intermediate blockage as its active sites are mobile [142]. Gilija and his labmates prepared PANI/TiO_2 nanocomposites in various ratios for photocatalysis and 15PANI/TiO_2 were found most suitable having the smallest homogenous particles of PANI. These presented the highest photocatalytic efficiency under ultraviolet A (UVA) irradiation as compared to pure TiO_2 and it can be explained by the establishment of uniformly dispersed PANI chains on the TiO_2nanoparticles that was found responsible for the synergistic PANI–TiO_2 effect [143]. The surface of TiO_2 has been protected from the blockage of intermediates by the PANI present in the composite which is due to the enhanced photocatalytic performance of 15PANI/TiO_2 as compared to TiO_2. The photocatalyst process is facilitated by PANI which allows the PANI–TiO_2 synergetic effect and hence can reduce the recombination process of electron and holes in TiO_2. In situ chemical oxidation of aniline results in the preparation of photocatalyst of PANI/TiO_2 composite. It was observed that the concentration of aniline depends upon the photocatalytic properties, morphology, and aggregation processes (Scheme 2). With the increase in the concentration of aniline, the conductivity of composites did not increase linearly [123].

As a result, it has been observed that 15PANI/TiO_2 composite demineralized 80% whereas pure TiO_2 demineralized only 35% of RR45 dye. The higher photoactivity efficiency of the composite catalysts has been explained by the achieved PANI–TiO_2

Scheme 1 Photocatalytic degradation of Malachite green

$$TiO_2 \xrightarrow{h\upsilon} h^+ + e^-$$
$$h^+ + e^- \xrightarrow{h\upsilon} \text{heat}$$
$$MG^+ + H^+ + 2e^- \xrightarrow{K_1} MGH^-(leuco)$$
$$MGH^-(leuco) \longrightarrow NH_4 + CO_2$$

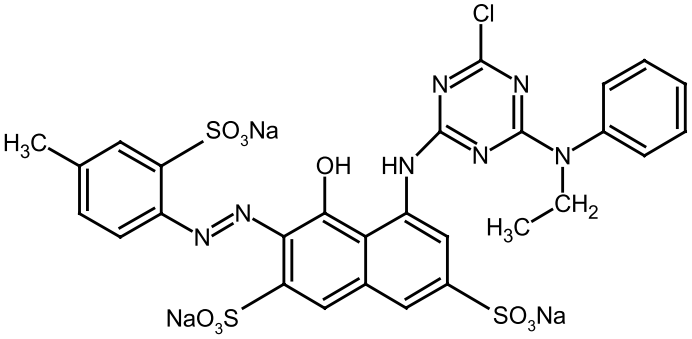

Scheme 2 Structure of RR45 dye

synergistic effect. The PANI–TiO_2 synergistic effect was additionally confirmed by UV/Vis photocatalysis, as 15PANI/TiO_2 (vs. pure TiO_2) yielded a more efficient catalytic process. To gain a deeper insight into the photocatalytic process of wastewater purification by 15PANI/TiO_2 composite, it is necessary to further investigate the efficiency of water load, degradation kinetics as well as modeling of the system to achieve optimal experimental conditions [144].

Degradation of rhodamine B (RB)

The common method has been used for the preparation of nanocomposite catalysts of TiO_2/PANI was given by Reddy [145]. Solgel method and hydrothermal process with some modification have been used for the preparation of TiO_2 NPs at 550 °C. Nanocomposites have been prepared without utilizing TiO_2 by using pristine PANI under the same conditions required for the solgel method. TiO_2/PANI-0, TiO_2/PANI-5, TiO_2/PANI-10, TiO_2/PANI-15, and TiO_2/PANI-20 were used for denoting the nanocomposite catalyst of TiO_2/PANI. Different weight % of TiO_2 was used for the investigation of photocatalytic activity of the TiO_2/PANI and TiO_2 nanoparticle. The rate of decomposition of RB dye has been used for the evaluation of the composite catalysts of TiO_2/PANI. The rate of degradation of RB dye was high in the presence of nanocomposite of TiO_2/PANI-20. A plot of –ln(Co/C) vs. time for 20% concentration of hybrid catalyst of TiO_2/PANI has been drawn and it has been observed that 0.954 is the regression coefficient and the equation follows first-order degradation kinetics and the rate constant of the reaction was 0.007642 min^{-1}.

Photocatalytic degradation of methylene blue has been observed in the presence of hybrid catalyst TiO_2/PANI-20 and nanoparticle of TiO_2 under UV light. In the absence of photocatalyst, the black test was carried out under irradiation with UV. Minimum methylene blue degradation was shown by the photocatalytic test whereas 27% methylene blue degradation in the presence of nanoparticle of TiO_2 when exposed to UV irradiation. On the other hand, 73% of methylene blue was degraded in the presence of nanocomposite of TiO_2/PANI (Fig. 12). Synergistic effect results in greater photocatalytic activity of the composite catalysts of TiO_2/PANI. The rate of degradation of dye in the presence of nanoparticle of TiO_2 and composite

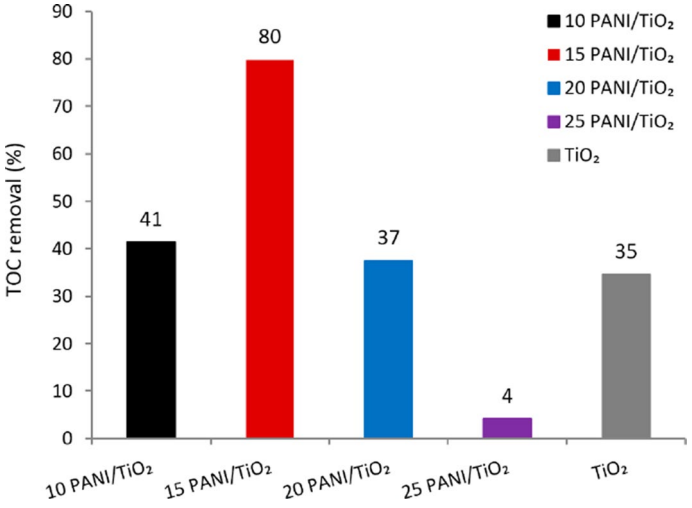

Fig. 12 RR 45 dye removal after 90 min of photocatalysis with TiO_2 and PANI/TiO_2. Reproduced from nanomaterials, Vol. 7(12), pp. 412, Vanja Gilja, Katarina Novakovi, Jadranka Travas-Sejdic, Zlata Hrnjak-Murgi, Marijana Kralji Rokovi and Mark Žic, Stability and Synergistic Effect of Polyaniline/TiO_2 Photocatalysts in Degradation of Azo Dye in Wastewater © 2017 with permission of MDPI

catalyst of TiO_2/PANI-20 has been observed by a plot ln(C/Co) vs. time and it was observed that it follows first-order degradation kinetics for hybrid catalyst and 0.95 is the regression coefficient. The observed value for the regression coefficient was equivalent to the experimental data [115, 145]. A photolytic degradation mechanism of Rhodamine B by PANI/TiO_2 was proposed by Jing Ma and his labmates based on the results obtained, Fig. 13. They discussed the LUMO and HOMO potential gap of PANI was higher as compared to the conduction band and the Valence band of TiO_2 revealed that HOMO of PANI is in between conduction ad valence band of TiO_2. When light irradiated, PANI and TiO_2 generated electron–hole pair. The holes generated in the valence band of TiO_2 injected in HOMO of PANI, while the electrons generated at LUMO of PANI at the same time transfer to the conduction band of TiO_2. Therefore, a charge separation occurred and stopped electron–hole recombination at the surface of nanocomposites and promotes photocatalytic activity. The migrated electrons at the conduction band of TiO_2 oxidatively interacts with the surface oxygen to yield superoxide anion radicals ($\cdot O2^{-}$) as well as the holes at HOMO of PANI reacts with water to generate hydroxyl radical ($OH^{\cdot}$). These superoxide anion radical and hydroxyl radicals are responsible for photocatalytic dye degradation of Rhodamine B by PANI/TiO_2 nanocomposites [146].

To investigate the reusability of catalysts, TiO_2 and the composite of TiO_2/PANI undergo three photocatalytic cycles to examine the reusability of the catalyst and every cycle lasts for 3 h 20 min. The catalyst obtained by photocatalytic reaction without any treatment was utilized for an additional two runs after its separation. 34% of RhB was degraded by TiO_2 particles in 3 h 20 min after 3 cycles. It was observed that the degradation of phenol and methyl blue was 28% and 24% after three cycles and 51% and 67% was the activity of composite

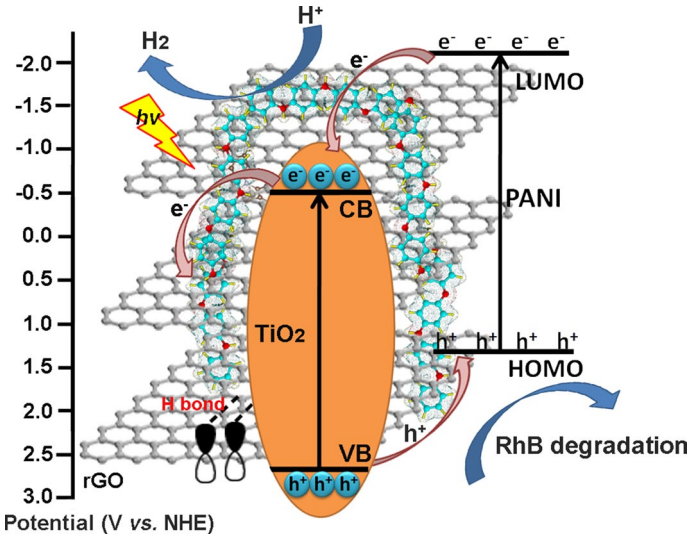

Fig. 13 Schematic representation of Rhodamine B dye degradation using PANI/TiO_2 nanocomposites. Reproduced from Renewable Energy, Vol. 156, pp. 1008–1018, Ma, Jing, Jianan Dai, Yinli Duan, Jiajia Zhang, Liangsheng Qiang, and Juanqin Xue. "Fabrication of PANI–TiO_2/rGO hybrid composites for enhanced photocatalysis of pollutant removal and hydrogen production." © 2020 with permission of Elsevier

catalyst of TiO_2/PANI for the degradation of phenol and methyl blue at 3 h 20 min irradiation time. Hence it was observed that the composite catalysts exhibit reusable property. From these observations, it was observed that the efficiency of degradation of three pollutants using composite catalysts of TiO_2/PANI is considerably higher as compared to pure TiO_2 in 2 h of UV irradiation time. The probable reasons for improved activity are-

(i) Coupling of PANI and TiO_2 results in the effective charge separation of photogenerated holes and electrons.
(ii) The rate of dispersion of TiO_2 nanoparticles (NPs) increases in the composite of TiO_2/PANI which increases the catalytic activity of the composite catalyst. This result leads to more adsorption of molecules of dye onto the catalyst's surface. Hence, it results in stronger interaction between the dye solution and the composite catalyst of TiO_2/PANI.
(iii) Different optical behavior was exhibited by the composite catalysts of TiO_2/PANI as compared to NPs of pristine TiO_2. Besides the absorption of UV light, the composite catalyst can also absorb visible and near-IR light. The adsorption of the light is responsible for the increase in the photoactive region of NPs of TiO_2 and hence the observation indicates that the PANI is an outstanding photosensitizer for TiO_2 nanoparticle.
(iv) The photocatalytic activity of composite increases due to the modification of PANI onto the TiO_2 nanoparticle.

(v) The results indicate that the rate constant for TiO_2 coated with PANI is improved as compared to pure TiO_2. Hence, the efficiency of degradation of methylene blue, RB, and phenol is greater for the composite catalyst of TiO_2/PANI.

In-situ chemical oxidative polymerization technique was used for the synthesis of PANI-modified TiO_2 and its photocatalytic, structural, and morphological properties were characterized. The photocatalytic activity of photocatalysts is higher than the unmodified TiO_2 for the degradation of dyes. After 180 min of irradiation, it was observed that more than 80% of the RB was degraded by using the composite catalyst of TiO_2/PANI with 20% of TiO_2. 0.007642 min^{-1} is the rate constant for 20% nanocomposite of TiO_2/PANI. It was observed that the rate of degradation of pollutants by composite catalyst was higher as compared to pristine TiO_2. 0.0038 & 0.00684 min^{-1} are the rate constant for phenol and methylene blue. Thus, this work gives an idea for the preparation of TiO_2 modified with another electron-donating functional material (e.g., porous carbons, graphene nanosheets, carbon nitride, reduced graphene oxide, one-dimensional carbon nanofibers, quantum dots, etc.) or organic conjugated polymers such as polythiophene, polytoluidine, polyanisidine, etc. [147].

Comparison of the effectiveness of degradation between PANI–TiO_2 with other compounds

PANI has a narrow bandgap of 2.8 eV which is an outstanding candidate to sensitize TiO_2 nanoparticles having a bandgap of 3.2 eV. The superior photocatalysis of dye with PANI/TiO_2 nanocomposites ascribed to the sufficient electron–hole charge separation and electrons from π–π* absorption band of PANI transferred to the conduction band of TiO_2 nanoparticles and holes created on valence band of TiO2 got transferred to HOMO of PANI. Therefore, in the valence band, there is an excess of the hole which produces hydroxyl and superoxide radicals on the surface of TiO_2, to increase photocatalytic activity [148, 149]. The decoloration efficiency for dye degradation by nanocomposites was found 98.6% as compared to pristine PANI and TiO_2 [150].

Many researchers synthesized nanocomposites of PANI with ZnO (zinc oxide) having a bandgap of 3.37 eV which is wide as compared to TiO_2. However, ZnO is too inexpensive but it is superior to TiO_2 for commercial consideration. Saravanan et al. [64] prepared PANI/ZnO nanocomposites for effective visible-light photocatalytic degradation of methyl orange and methylene blue dyes. When the nanocomposite surface was illuminated by light then intermolecular interaction between ZnO and PANI took place. When PANI was excited about π–π* transition of electrons then electrons from LUMO of PANI transferred to the conduction band of ZnO which resulted in the formation of superoxide anion radical and hydroxyl radical, responsible for photocatalytic dye degradation. The coupling of ZnO with PANI effectiveness of photocatalysis is effective in natural sunlight too. In this regard, nanocomposites of PANI/ZnO were analyzed and resulted in 99% efficiency for dye degradation after 5 h of irradiation under natural sunlight [151].

In case of PPy/TiO_2 nanocomposites, the degradation of methylene blue dye increased to 74.08% after 1 h of UV exposure, while in case of pristine PPy, it was found only 8.47% in absence of TiO_2, while some other researchers reported that 50% decay in absorbance of dye degradation in the presence of PPy film containing TiO2 as compared to pristine PPy, i.e., 1.4% [152]. The methyl orange dye degradation with PTh/TiO_2 was found to 56.6% after 3 h of UV exposure. The decolorization of methyl orange for TiO_2 and its composites with PANI in various molar ratios were calculated to be 77.6, 90.1, 92.7, and 86.8 respectively which indicated enhanced photocatalytic degradation of dye in presence of polythiophene.

Conclusion

This review reveals that PANI act as an effective sensitizer for TiO_2 nanoparticles. The performance of PANI-sensitized TiO_2 nanocomposite is depended on various structural parameters. The efficiency of the separation of photogenerated electrons should be sensitively varied by the interfacial interactions between the PANI backbone and the substrates of oxide. For enhancement of photocatalytic activity, covalent bonding promotes the electronic coupling which is beneficial for electron injection from the PANI excited state into the CB of TiO_2. The structures of the dye molecules also affect the electron transfer at the interface between the dyes and the nanocomposite surface. Since the photocatalytic activity of these materials depends on their light-responsive range and carrier-separation capacity. PANI–TiO_2-based photocatalysis has been used for their potential application in environmental remediation with special emphasis on methylene blue and rhodamine B dyes. This review concluded that PANI/TiO_2 nanocomposites are highly efficient photocatalytic materials for degrading contaminated colored wastewater for reuse in textile industries under mild conditions.

Acknowledgements The authors are thankful to the American Chemical Society, Elsevier, Springer and Taylor & Francis for copyright permission.

Compliance with ethical standards

Conflict of interest There is no conflict of interest.

References

1. Li X, Wang D, Cheng G et al (2008) Preparation of polyaniline-modified TiO_2 nanoparticles and their photocatalytic activity under visible light illumination. Appl Catal B 81:267–273
2. Wu J-M, Zhang T-W (2004) Photodegradation of rhodamine B in water assisted by titania films prepared through a novel procedure. J Photochem Photobiol, A 162:171–177
3. Dodd A, McKinley A, Saunders M, Tsuzuki T (2006) Mechanochemical synthesis of nanocrystalline SnO_2–ZnO photocatalysts. Nanotechnology 17:692
4. Bansal P, Bhullar N, Sud D (2009) Studies on photodegradation of malachite green using TiO_2/ZnO photocatalyst. Desalin Water Treat 12:108–113

5. Chen CC, Lu CS, Chung YC, Jan JL (2007) UV light induced photodegradation of malachite green on TiO_2 nanoparticles. J Hazard Mater 141:520–528
6. Kominami H, Kumamoto H, Kera Y, Ohtani B (2003) Photocatalytic decolorization and mineralization of malachite green in an aqueous suspension of titanium (IV) oxide nano-particles under aerated conditions: correlation between some physical properties and their photocatalytic activity. J Photochem Photobiol, A 160:99–104
7. Karunakaran C, Senthilvelan S (2005) Photocatalysis with ZrO_2: oxidation of aniline. J Mol Catal A: Chem 233:1–8
8. Kakuta S, Abe T (2009) Photocatalysis for water oxidation by Fe_2O_3 nanoparticles embedded in clay compound: correlation between its polymorphs and their photocatalytic activities. J Mater Sci 44:2890–2898
9. Pawar RC, Khare V, Lee CS (2014) Hybrid photocatalysts using graphitic carbon nitride/cadmium sulfide/reduced graphene oxide (gC_3N_4/CdS/RGO) for superior photodegradation of organic pollutants under UV and visible light. Dalton Trans 43:12514–12527
10. Gurr J-R, Wang ASS, Chen C-H, Jan K-Y (2005) Ultrafine titanium dioxide particles in the absence of photoactivation can induce oxidative damage to human bronchial epithelial cells. Toxicology 213:66–73
11. Xing Z, Zhang J, Cui J et al (2018) Recent advances in floating TiO_2-based photocatalysts for environmental application. Appl Catal B 225:452–467
12. Fujishima A, Zhang X, Tryk DA (2008) TiO_2 photocatalysis and related surface phenomena. Surf Sci Rep 63:515–582
13. Fujishima A, Honda K (1972) Electrochemical photolysis of water at a semiconductor electrode. Nature 238:37–38
14. Chatterjee D, Dasgupta S (2005) Visible light induced photocatalytic degradation of organic pollutants. J Photochem Photobiol, C 6:186–205
15. Konstantinou IK, Albanis TA (2004) TiO_2-assisted photocatalytic degradation of azo dyes in aqueous solution: kinetic and mechanistic investigations: a review. Appl Catal B 49:1–14
16. Kumar SG, Devi LG (2011) Review on modified TiO_2 photocatalysis under UV/visible light: selected results and related mechanisms on interfacial charge carrier transfer dynamics. J Phys Chem A 115:13211–13241
17. Natarajan TS, Natarajan K, Bajaj HC, Tayade RJ (2013) Enhanced photocatalytic activity of bismuth-doped TiO_2 nanotubes under direct sunlight irradiation for degradation of Rhodamine B dye. J Nanopart Res 15:1669
18. Schneider J, Matsuoka M, Takeuchi M et al (2014) Understanding TiO_2 photocatalysis: mechanisms and materials. Chem Rev 114:9919–9986
19. Tayade RJ, Surolia PK, Kulkarni RG, Jasra RV (2007) Photocatalytic degradation of dyes and organic contaminants in water using nanocrystalline anatase and rutile TiO_2. Sci Technol Adv Mater 8:455
20. Su C, Hong B-Y, Tseng C-M (2004) Sol–gel preparation and photocatalysis of titanium dioxide. Catal Today 96:119–126
21. Yan M, Chen F, Zhang J, Anpo M (2005) Preparation of controllable crystalline titania and study on the photocatalytic properties. J Phys Chem B 109:8673–8678
22. Lin H, Huang CP, Li W et al (2006) Size dependency of nanocrystalline TiO_2 on its optical property and photocatalytic reactivity exemplified by 2-chlorophenol. Appl Catal B 68:1–11
23. Pekakis PA, Xekoukoulotakis NP, Mantzavinos D (2006) Treatment of textile dyehouse wastewater by TiO_2 photocatalysis. Water Res 40:1276–1286
24. Marin ML, Santos-Juanes L, Arques A et al (2011) Organic photocatalysts for the oxidation of pollutants and model compounds. Chem Rev 112:1710–1750
25. Meng Z-D, Zhu L, Choi J-G et al (2011) Effect of Pt treated fullerene/TiO_2 on the photocatalytic degradation of MO under visible light. J Mater Chem 21:7596–7603
26. Rodríguez AL, Gallardo PS, Rivera MÁH et al (2012) Photocatalytic degradation of methylene blue dye in aqueous solutions by photocatalytic oxidation SiO_2–TiO_2. Adv Sci Lett 13:841–843
27. Chowdhury P, Moreira J, Gomaa H, Ray AK (2012) Visible-solar-light-driven photocatalytic degradation of phenol with dye-sensitized TiO_2: parametric and kinetic study. Ind Eng Chem Res 51:4523–4532
28. Dresselhaus M, Dresselhaus G, Cronin SB, Souza Filho AG (2018) Absorption of light in solids. In: Solid state properties. Springer, Berlin, pp 365–389

29. Qamar A, Amin MR, Grynko O et al (2019) A probe of valence and conduction band electronic structure of lead oxide films for photodetectors. ChemPhysChem 20:3328–3335. https://doi.org/10.1002/cphc.201900726
30. Tsai C-Y (2019) The effects of intraband and interband carrier-carrier scattering on hot-carrier solar cells: a theoretical study of spectral hole burning, electron-hole energy transfer, Auger recombination, and impact ionization generation. Prog Photovoltaics Res Appl 27:433–452. https://doi.org/10.1002/pip.3116
31. Bayer M, Stern O, Hawrylak P et al (2000) Hidden symmetries in the energy levels of excitonic 'artificial atoms'. Nature 405:923–926. https://doi.org/10.1038/35016020
32. Patsoura A, Kondarides DI, Verykios XE (2006) Enhancement of photoinduced hydrogen production from irradiated Pt/TiO_2 suspensions with simultaneous degradation of azo-dyes. Appl Catal B 64:171–179. https://doi.org/10.1016/j.apcatb.2005.11.015
33. Zangeneh H, Zinatizadeh AAL, Habibi M et al (2015) Photocatalytic oxidation of organic dyes and pollutants in wastewater using different modified titanium dioxides: a comparative review. J Ind Eng Chem 26:1–36. https://doi.org/10.1016/j.jiec.2014.10.043
34. Bahnemann D (2004) Photocatalytic water treatment: solar energy applications. Sol Energy 77:445–459. https://doi.org/10.1016/j.solener.2004.03.031
35. Paz Y (2010) Application of TiO_2 photocatalysis for air treatment: patents' overview. Appl Catal B 99:448–460. https://doi.org/10.1016/j.apcatb.2010.05.011
36. Li Y, Wang W, Qiu X et al (2011) Comparing Cr, and N only doping with (Cr, N)-codoping for enhancing visible light reactivity of TiO_2. Appl Catal B 110:148–153. https://doi.org/10.1016/j.apcatb.2011.08.037
37. Wang H, Zhang L, Chen Z et al (2014) Semiconductor heterojunction photocatalysts: design, construction, and photocatalytic performances. Chem Soc Rev 43:5234–5244. https://doi.org/10.1039/C4CS00126E
38. Bingham S, Daoud WA (2011) Recent advances in making nano-sized TiO_2 visible-light active through rare-earth metal doping. J Mater Chem 21:2041–2050. https://doi.org/10.1039/C0JM02271C
39. Jadoun S, Sharma V, Ashraf SM, Riaz U (2017) Sonolytic doping of poly(1-naphthylamine) with luminol: influence on spectral, morphological and fluorescent characteristics. Colloid Polym Sci. https://doi.org/10.1007/s00396-017-4055-3
40. Riaz U, Ashraf SM, Kumar Saroj S et al (2016) Microwave-assisted solid state intercalation of Rhodamine B and polycarbazole in bentonite clay interlayer space: structural characterization and photophysics of double intercalation. RSC Adv. https://doi.org/10.1039/c5ra27387k
41. Riaz U, Jadoun S, Kumar P et al (2017) Influence of luminol doping of poly(o-phenylenediamine) on the spectral, morphological, and fluorescent properties: a potential fluorescent marker for early detection and diagnosis of Leishmania donovani. ACS Appl Mater Interfaces. https://doi.org/10.1021/acsami.7b10325
42. Jadoun S, Ashraf SM, Riaz U (2018) Microwave-assisted synthesis of copolymers of luminol with anisidine: effect on spectral, thermal and fluorescence characteristics. Polym Adv Technol 29:1007–1017
43. Riaz U, Jadoun S, Kumar P et al (2018) Microwave-assisted facile synthesis of poly (luminol-co-phenylenediamine) copolymers and their potential application in biomedical imaging. RSC Adv 8:37165–37175
44. Riaz U, Ashraf SM, Jadoun S et al (2019) Spectroscopic and biophysical interaction studies of water-soluble dye modified poly (o-phenylenediamine) for its potential application in BSA detection and bioimaging. Sci Rep 9:8544
45. Jadoun S, Riaz U (2019) A review on the chemical and electrochemical copolymerization of conducting monomers: recent advancements and future prospects. Polym-Plast Technol Mater 1–21
46. Das TK, Prusty S (2012) Review on conducting polymers and their applications. Polym-Plast Technol Eng 51:1487–1500. https://doi.org/10.1080/03602559.2012.710697
47. Riaz U, Ashraf SM, Aleem S et al (2016) Microwave-assisted green synthesis of some nano-conjugated copolymers: characterisation and fluorescence quenching studies with bovine serum albumin. New J Chem. https://doi.org/10.1039/c5nj02513c
48. Jadoun S, Riaz U (2020) Conjugated polymer light-emitting diodes. Polym Light-Emit Dev Displays. https://doi.org/10.1002/9781119654643.ch4

49. Jadoun S, Riaz U (2020) A review on the chemical and electrochemical copolymerization of conducting monomers: recent advancements and future prospects. Polym-Plast Technol Mater 59:484–504. https://doi.org/10.1080/25740881.2019.1669647
50. Kumari Jangid N, Jadoun S, Kaur N (2020) A review on high-throughput synthesis, deposition of thin films and properties of polyaniline. Eur Polym J 125:109485. https://doi.org/10.1016/j.eurpolymj.2020.109485
51. Riaz U, Ashraf SM (2015) Microwave-induced catalytic degradation of a textile dye using bentonite–poly(o-toluidine) nanohybrid. RSC Adv 5:3276–3285. https://doi.org/10.1039/C4RA08054H
52. Le T-H, Kim Y, Yoon H (2017) Electrical and electrochemical properties of conducting polymers. Polymers. https://doi.org/10.3390/polym9040150
53. Jadoun S, Verma A, Ashraf SM, Riaz U (2017) A short review on the synthesis, characterization, and application studies of poly(1-naphthylamine): a seldom explored polyaniline derivative. Colloid Polym Sci. https://doi.org/10.1007/s00396-017-4129-2
54. Jadoun S, Biswal L, Riaz U (2018) Tuning the optical properties of poly(o-phenylenediamine-co-pyrrole) via template mediated copolymerization. Des Monomers Polym 21:75–81. https://doi.org/10.1080/15685551.2018.1459078
55. Jadoun S, Ashraf SM, Riaz U (2017) Tuning the spectral, thermal and fluorescent properties of conjugated polymers: via random copolymerization of hole transporting monomers. RSC Adv 7:32757–32768. https://doi.org/10.1039/c7ra04662f
56. Jadoun S, Verma A, Riaz U (2018) Luminol modified polycarbazole and poly (o-anisidine): Theoretical insights compared with experimental data. Spectrochim Acta Part A: Mol Biomol Spectrosc
57. Riaz U, Ashraf SM, Fatima T, Jadoun S (2017) Spectrochimica Acta Part A: molecular and biomolecular spectroscopy tuning the spectral, morphological and photophysical properties of sonochemically synthesized poly (carbazole) using acid Orange, fl uorescein and rhodamine 6G. SAA 173:986–993. https://doi.org/10.1016/j.saa.2016.11.003
58. Riaz U, Ahmad S, Ashraf SM (2008) Pseudo template synthesis of poly (1-naphthylamine): effect of environment on nanostructured morphology. J Nanopart Res 10:1209–1214. https://doi.org/10.1007/s11051-007-9356-x
59. Awuzie CI (2017) Conducting polymers. Mater Today: Proc 4:5721–5726. https://doi.org/10.1016/j.matpr.2017.06.036
60. Riaz U, Ahmad S, Ashraf SM (2009) Effect of solvent on the characteristics of nanostructured composites of poly (1-naphthylamine) with poly (vinyl alcohol). Curr Appl Phys 9:581–587. https://doi.org/10.1016/j.cap.2008.05.012
61. Fratoddi I, Venditti I, Cametti C, Russo MV (2015) Chemiresistive polyaniline-based gas sensors: a mini review. Sens Actuators B: Chem 220:534–548. https://doi.org/10.1016/j.snb.2015.05.107
62. Ansari AA, Khan MAM, Khan MN et al (2011) Optical and electrical properties of electrochemically deposited polyaniline/CeO_2 hybrid nanocomposite film. J Semicond 32:43001. https://doi.org/10.1088/1674-4926/32/4/043001
63. Shimano JY, MacDiarmid AG (2001) Polyaniline, a dynamic block copolymer: key to attaining its intrinsic conductivity? Synth Met 123:251–262. https://doi.org/10.1016/S0379-6779(01)00293-4
64. Saravanan R, Sacari E, Gracia F et al (2016) Conducting PANI stimulated ZnO system for visible light photocatalytic degradation of coloured dyes. J Mol Liq 221:1029–1033. https://doi.org/10.1016/j.molliq.2016.06.074
65. Wang L, Feng X, Ren L et al (2015) Flexible solid-state supercapacitor based on a metal-organic framework interwoven by electrochemically-deposited PANI. J Am Chem Soc 137:4920–4923. https://doi.org/10.1021/jacs.5b01613
66. Liu P, Huang Y, Yan J, Zhao Y (2016) Magnetic graphene@PANI@porous TiO_2 ternary composites for high-performance electromagnetic wave absorption. J Mater Chem C 4:6362–6370. https://doi.org/10.1039/C6TC01718E
67. Kashyap G, Ameta G, Ameta C et al (2019) Synthesis and characterization of polyaniline-drug conjugates as effective antituberculosis agents. Bioorg Med Chem Lett 29:1363–1369. https://doi.org/10.1016/j.bmcl.2019.03.040
68. Jangid NK, Chauhan NPS, Punjabi PB (2015) Preparation and characterization of polyanilines bearing rhodamine 6-G and Azure B as pendant groups. J Macromol Sci Part A 52:95–104. https://doi.org/10.1080/10601325.2015.980714
69. Israr H, Rasool N, Rizwan K et al (2019) Synthesis and reactivities of triphenyl acetamide analogs for potential nonlinear optical material uses. Symmetry. https://doi.org/10.3390/sym11050622

70. Jangid NK, Chauhan NPS, Punjabi PB (2014) Novel dye-substituted polyanilines: conducting and antimicrobial properties. Polym Bull 71:2611–2630. https://doi.org/10.1007/s00289-014-1210-6
71. Jangid NK, Chauhan NPS, Ameta C et al (2014) Synthesis and characterization of functionalized polyaniline having methyl violet as pendant groups. J Macromol Sci Part A 51:625–632. https://doi.org/10.1080/10601325.2014.924835
72. Chauhan NPS, Jangid NK, Punjabi PB (2013) Synthesis and characterization of conducting polyanilines via catalytic oxidative polymerization. Int J Polym Mater Polym Biomater 62:550–555. https://doi.org/10.1080/00914037.2012.761625
73. Tai H, Jiang Y, Xie G et al (2008) Influence of polymerization temperature on NH_3 response of PANI/TiO_2 thin film gas sensor. Sens Actuators B: Chem 129:319–326
74. Liu C, Tai H, Zhang P et al (2017) Enhanced ammonia-sensing properties of PANI–TiO_2–Au ternary self-assembly nanocomposite thin film at room temperature. Sens Actuators B: Chem 246:85–95
75. Yang C, Dong W, Cui G et al (2017) Enhanced photocatalytic activity of PANI/TiO_2 due to their photosensitization-synergetic effect. Electrochim Acta 247:486–495
76. Yu J, Pang Z, Zheng C et al (2019) Cotton fabric finished by PANI/TiO_2 with multifunctions of conductivity, anti-ultraviolet and photocatalysis activity. Appl Surf Sci 470:84–90
77. Bian C, Yu Y, Xue G (2007) Synthesis of conducting polyaniline/TiO_2 composite nanofibres by one-step in situ polymerization method. J Appl Polym Sci 104:21–26
78. Zhang L, Liu P, Su Z (2006) Preparation of PANI–TiO_2 nanocomposites and their solid-phase photocatalytic degradation. Polym Degrad Stab 91:2213–2219. https://doi.org/10.1016/j.polymdegradstab.2006.01.002
79. Sui X, Chu Y, Xing S, Liu C (2004) Synthesis of PANI/AgCl, PANI/BaSO4 and PANI/TiO_2 nanocomposites in CTAB/hexanol/water reverse micelle. Mater Lett 58:1255–1259. https://doi.org/10.1016/j.matlet.2003.09.035
80. Tai H, Jiang Y, Xie G, Yu J (2010) Preparation, characterization and comparative NH_3-sensing characteristic studies of PANI/inorganic oxides nanocomposite thin films. J Mater Sci Technol 26:605–613. https://doi.org/10.1016/S1005-0302(10)60093-X
81. Ansari MO, Mohammad F (2011) Thermal stability, electrical conductivity and ammonia sensing studies on p-toluenesulfonic acid doped polyaniline:titanium dioxide (pTSA/Pani:TiO_2) nanocomposites. Sens Actuators B: Chem 157:122–129. https://doi.org/10.1016/j.snb.2011.03.036
82. Su B, Min S, She S et al (2007) Synthesis and characterization of conductive polyaniline/TiO_2 composite nanofibers. Front Chem China 2:123–126. https://doi.org/10.1007/s11458-007-0025-5
83. Zhang L, Wan M, Wei Y (2005) Polyaniline/TiO_2 microspheres prepared by a template-free method. Synth Met 151:1–5. https://doi.org/10.1016/j.synthmet.2004.12.021
84. Cheng Y, An L, Zhao Z, Wang G (2014) Preparation of polyaniline/TiO_2 composite nanotubes for photodegradation of AZO dyes. J Wuhan Univ Technol-Mater Sci Ed 29:468–472. https://doi.org/10.1007/s11595-014-0941-4
85. Jumat NA, Wai PS, Ching JJ, Basirun WJ (2017) Synthesis of polyaniline-TiO_2 nanocomposites and their application in photocatalytic degradation. Polym Polym Compos 25:507–514
86. Zhang L, Wan M (2003) Polyaniline/TiO_2 composite nanotubes. J Phys Chem B 107:6748–6753
87. Sui X, Chu Y, Xing S et al (2004) Self-organization of spherical PANI/TiO_2 nanocomposites in reverse micelles. Colloids Surf A 251:103–107
88. Xiong S, Wang Q, Xia H (2004) Template synthesis of polyaniline/TiO_2 bilayer microtubes. Synth Met 146:37–42
89. Nabid MR, Golbabaee M, Moghaddam AB et al (2008) Polyaniline/TiO_2 nanocomposite: enzymatic synthesis and electrochemical properties. Int J Electrochem Sci 3:1117–1126
90. Nabid MR, Sedghi R, Moghaddam AB et al (2009) Synthesis of polyaniline/TiO_2 nanocomposites with metalloporphyrin and metallophthalocyanine catalysts. J Porphyrins Phthalocyanines 13:980–985
91. Katoch A, Burkhart M, Hwang T, Kim SS (2012) Synthesis of polyaniline/TiO_2 hybrid nanoplates via a sol–gel chemical method. Chem Eng J 192:262–268. https://doi.org/10.1016/j.cej.2012.04.004
92. Pawar SG, Patil SL, Chougule MA et al (2010) Synthesis and characterization of polyaniline:TiO_2 nanocomposites. Int J Polym Mater Polym Biomater 59:777–785. https://doi.org/10.1080/00914037.2010.483217

93. Chen F, An W, Li Y et al (2018) Fabricating 3D porous PANI/TiO_2–graphene hydrogel for the enhanced UV-light photocatalytic degradation of BPA. Appl Surf Sci 427:123–132. https://doi.org/10.1016/j.apsusc.2017.08.146
94. Gu L, Wang J, Qi R et al (2012) A novel incorporating style of polyaniline/TiO_2 composites as effective visible photocatalysts. J Mol Catal A: Chem 357:19–25. https://doi.org/10.1016/j.molcata.2012.01.012
95. Ma Y, Zhang C, Hou C et al (2017) Cetyl trimethyl ammonium bromide (CTAB) micellar templates directed synthesis of water-dispersible polyaniline rhombic plates with excellent processability and flow-induced color variation. Polymer 117:30–36. https://doi.org/10.1016/j.polymer.2017.04.010
96. Kumar R, Yadav BC (2016) Humidity sensing investigation on nanostructured polyaniline synthesized via chemical polymerization method. Mater Lett 167:300–302
97. Hashemi Monfared A, Jamshidi M (2019) Synthesis of polyaniline/titanium dioxide nanocomposite (PAni/TiO_2) and its application as photocatalyst in acrylic pseudo paint for benzene removal under UV/VIS lights. Prog Org Coat 136:105257. https://doi.org/10.1016/j.porgcoat.2019.105257
98. Zhu C, Cheng X, Dong X (2018) Enhanced Sub-ppm NH_3 gas sensing performance of PANI/TiO_2 nanocomposites at room temperature. Front Chem 6:493
99. Gawri I, Ridhi R, Singh KP, Tripathi SK (2018) Chemically synthesized TiO_2 and PANI/TiO_2 thin films for ethanol sensing applications. Mater Res Express 5:25303. https://doi.org/10.1088/2053-1591/aaa9f1
100. Gawri I, Ridhi R, Singh KP, Tripathi SK (2018) Chemically synthesized TiO_2 and PANI/TiO_2 thin films for ethanol sensing applications. Mater Rese Express 5:25303
101. Wang F, Min SX (2007) TiO_2/polyaniline composites: an efficient photocatalyst for the degradation of methylene blue under natural light. Chin Chem Lett 18:1273–1277. https://doi.org/10.1016/j.cclet.2007.08.010
102. Wang N, Chen J, Wang J et al (2019) Removal of methylene blue by polyaniline/TiO_2 hydrate: adsorption kinetic, isotherm and mechanism studies. Powder Technol 347:93–102. https://doi.org/10.1016/j.powtec.2019.02.049
103. Wang F, Min S, Han Y, Feng L (2010) Visible-light-induced photocatalytic degradation of methylene blue with polyaniline-sensitized TiO_2 composite photocatalysts. Superlattices Microstruct 48:170–180. https://doi.org/10.1016/j.spmi.2010.06.009
104. Salem MA, Al-Ghonemiy AF, Zaki AB (2009) Photocatalytic degradation of Allura red and Quinoline yellow with polyaniline/TiO_2 nanocomposite. Appl Catal B 91:59–66. https://doi.org/10.1016/j.apcatb.2009.05.027
105. Olad ALI, Behboudi S, Entezami ALIA (2012) Preparation, characterization and photocatalytic activity of TiO_2/polyaniline core-shell nanocomposite. Bull Mater Sci 35:801–809. https://doi.org/10.1007/s12034-012-0358-7
106. Navas Díaz A, González García JA, Lovillo J (1997) Enhancer effect of fluorescein on the luminol-H_2O_2-horseradish peroxidase chemiluminescence: energy transfer process. J Biolumin Chemilumin 12:199–205. https://doi.org/10.1002/(SICI)1099-1271(199707/08)12:4%3c199:AID-BIO445%3e3.0.CO;2-U
107. Akpan UG, Hameed BH (2009) Parameters affecting the photocatalytic degradation of dyes using TiO_2-based photocatalysts: a review. J Hazard Mater 170:520–529
108. Jain R, Mathur M, Sikarwar S, Mittal A (2007) Removal of the hazardous dye rhodamine B through photocatalytic and adsorption treatments. J Environ Manag 85:956–964
109. Deng F, Min L, Luo X et al (2013) Visible-light photocatalytic degradation performances and thermal stability due to the synergetic effect of TiO_2 with conductive copolymers of polyaniline and polypyrrole. Nanoscale 5:8703–8710
110. Elsayed MA, Gobara M (2016) Enhancement removal of tartrazine dye using HCl-doped polyaniline and TiO_2-decorated PANI particles. Mater Res Express 3:85301
111. Prastomo N, Ayad M, Kawamura G, Matsuda A (2011) Synthesis and characterization of polyaniline nanofiber/TiO_2 nanoparticles hybrids. J Ceram Soc Jpn 119:342–345
112. Song X, Qin J, Li T, et al (2019) Efficient construction and enriched selective adsorption-photocatalytic activity of PVA/PANI/TiO_2 recyclable hydrogel by electron beam radiation. J Appl Polym Sci
113. Koysuren O, Koysuren HN (2019) Photocatalytic activity of polyaniline/Fe-doped TiO_2 composites by in situ polymerization method. J Macromol Sci Part A 56:267–276

114. Yu Q, Wang M, Chen H, Dai Z (2011) Polyaniline nanowires on TiO_2 nano/microfiber hierarchical nano/microstructures: preparation and their photocatalytic properties. Mater Chem Phys 129:666–672. https://doi.org/10.1016/j.matchemphys.2011.05.012
115. Ahmad R, Mondal PK (2012) Adsorption and photodegradation of methylene blue by using PAni/TiO_2 nanocomposite. J Dispersion Sci Technol 33:380–386
116. Radoičić M, Šaponjić Z, Janković IA et al (2013) Improvements to the photocatalytic efficiency of polyaniline modified TiO_2 nanoparticles. Appl Catal B 136–137:133–139. https://doi.org/10.1016/j.apcatb.2013.01.007
117. Li Y, Yu Y, Wu L, Zhi J (2013) Processable polyaniline/titania nanocomposites with good photocatalytic and conductivity properties prepared via peroxo-titanium complex catalyzed emulsion polymerization approach. Appl Surf Sci 273:135–143. https://doi.org/10.1016/j.apsusc.2013.01.213
118. Zhu Y, Xu S, Jiang L et al (2008) Synthesis and characterization of polythiophene/titanium dioxide composites. React Funct Polym 68:1492–1498. https://doi.org/10.1016/j.reactfunctpolym.2008.07.008
119. Zhang T, ki Oyama T, Horikoshi S et al (2002) Photocatalyzed N-demethylation and degradation of methylene blue in titania dispersions exposed to concentrated sunlight. Solar Energy Mater Solar Cells 73:287–303. https://doi.org/10.1016/S0927-0248(01)00215-X
120. Yuan L, Yu Z, Li C et al (2014) PANI-sensitized N-TiO_2 inverse opals with enhanced photoelectrochemical performance and photocatalytic activity. J Electrochem Soc 161:H332–H336
121. Jeong W-H, Amna T, Ha Y-M et al (2014) Novel PANI nanotube@TiO_2 composite as efficient chemical and biological disinfectant. Chem Eng J 246:204–210. https://doi.org/10.1016/j.cej.2014.02.054
122. Subramanian E, Subbulakshmi S, Murugan C (2014) Inter-relationship between nanostructures of conducting polyaniline and the photocatalytic methylene blue dye degradation efficiencies of its hybrid composites with anatase TiO_2. Mater Res Bull 51:128–135. https://doi.org/10.1016/j.materresbull.2013.12.006
123. Lin Y, Li D, Hu J et al (2012) Highly efficient photocatalytic degradation of organic pollutants by PANI-modified TiO_2 composite. J Phys Chem C 116:5764–5772. https://doi.org/10.1021/jp211222w
124. Liu Z, Miao Y-E, Liu M et al (2014) Flexible polyaniline-coated TiO_2/SiO_2 nanofiber membranes with enhanced visible-light photocatalytic degradation performance. J Colloid Interface Sci 424:49–55. https://doi.org/10.1016/j.jcis.2014.03.009
125. Leng C, Wei J, Liu Z et al (2013) Facile synthesis of PANI-modified $CoFe_2O_4$–TiO_2 hierarchical flower-like nanoarchitectures with high photocatalytic activity. J Nanopart Res 15:1643. https://doi.org/10.1007/s11051-013-1643-0
126. Zarrin S, Heshmatpour F (2018) Photocatalytic activity of TiO_2/Nb_2O_5/PANI and TiO_2/Nb_2O_5/RGO as new nanocomposites for degradation of organic pollutants. J Hazard Mater 351:147–159. https://doi.org/10.1016/j.jhazmat.2018.02.052
127. Jiménez M, Ignacio Maldonado M, Rodríguez EM et al (2015) Supported TiO_2 solar photocatalysis at semi-pilot scale: degradation of pesticides found in citrus processing industry wastewater, reactivity and influence of photogenerated species. J Chem Technol Biotechnol 90:149–157. https://doi.org/10.1002/jctb.4299
128. Ma J, Yang M, Sun Y et al (2014) Fabrication of Ag/TiO_2 nanotube array with enhanced photocatalytic degradation of aqueous organic pollutant. Physica E 58:24–29. https://doi.org/10.1016/j.physe.2013.11.006
129. Liu Y, Zeng G, Tang L et al (2015) Highly effective adsorption of cationic and anionic dyes on magnetic Fe/Ni nanoparticles doped bimodal mesoporous carbon. J Colloid Interface Sci 448:451–459. https://doi.org/10.1016/j.jcis.2015.02.037
130. Cheng L, Zhang S, Wang Y et al (2016) Ternary P25–graphene–Fe_3O_4 nanocomposite as a magnetically recyclable hybrid for photodegradation of dyes. Mater Res Bull 73:77–83. https://doi.org/10.1016/j.materresbull.2015.06.047
131. Zhou Q, Zhong Y-H, Chen X et al (2014) Mesoporous anatase TiO_2/reduced graphene oxide nanocomposites: a simple template-free synthesis and their high photocatalytic performance. Mater Res Bull 51:244–250. https://doi.org/10.1016/j.materresbull.2013.12.034
132. Sarmah S, Kumar A (2011) Photocatalytic activity of polyaniline-TiO_2 nanocomposites. Indian J Phys 85:713. https://doi.org/10.1007/s12648-011-0071-1

133. Serpone N, Maruthamuthu P, Pichat P et al (1995) Exploiting the interparticle electron transfer process in the photocatalysed oxidation of phenol, 2-chlorophenol and pentachlorophenol: chemical evidence for electron and hole transfer between coupled semiconductors. J Photochem Photobiol, A 85:247–255. https://doi.org/10.1016/1010-6030(94)03906-B
134. Moumeni O, Hamdaoui O, Pétrier C (2012) Sonochemical degradation of malachite green in water. Chem Eng Process 62:47–53. https://doi.org/10.1016/j.cep.2012.09.011
135. Perera SD, Mariano RG, Vu K et al (2012) Hydrothermal synthesis of graphene-TiO_2 nanotube composites with enhanced photocatalytic activity. ACS Catal 2:949–956. https://doi.org/10.1021/cs200621c
136. Zhang H, Zong R, Zhao J, Zhu Y (2008) Dramatic visible photocatalytic degradation performances due to synergetic effect of TiO_2 with PANI. Environ Sci Technol 42:3803–3807
137. Gilja V, Novaković K, Travas-Sejdic J et al (2017) Stability and synergistic effect of polyaniline/TiO_2 photocatalysts in degradation of azo dye in wastewater. Nanomaterials. https://doi.org/10.3390/nano7120412
138. Melinte V, Stroea L, Chibac-Scutaru LA (2019) Polymer nanocomposites for photocatalytic applications. Catalysts. https://doi.org/10.3390/catal9120986
139. Lee LS, Chang C-J (2019) Recent developments about conductive polymer based composite photocatalysts. Polymers. https://doi.org/10.3390/polym11020206
140. Umar M (2013) Photocatalytic degradation of organic pollutants in water. In: Rashed HAAE-MN (ed). IntechOpen, Rijeka, p Ch. 8
141. Gupta SM, Tripathi M (2011) A review of TiO_2 nanoparticles. Chin Sci Bull 56:1639. https://doi.org/10.1007/s11434-011-4476-1
142. Song E, Choi J-W (2013) Conducting polyaniline nanowire and its applications in chemiresistive sensing. Nanomaterials. https://doi.org/10.3390/nano3030498
143. Gilja V, Novaković K, Travas-Sejdic J et al (2017) Stability and synergistic effect of polyaniline/TiO_2 photocatalysts in degradation of azo dye in wastewater. NANO 7(12):412
144. Teli SB, Molina S, Sotto A et al (2013) Fouling resistant polysulfone–PANI/TiO_2 ultrafiltration nanocomposite membranes. Ind Eng Chem Res 52:9470–9479. https://doi.org/10.1021/ie401037n
145. Reddy KR, Karthik KV, Prasad SBB et al (2016) Enhanced photocatalytic activity of nanostructured titanium dioxide/polyaniline hybrid photocatalysts. Polyhedron 120:169–174. https://doi.org/10.1016/j.poly.2016.08.029
146. Ma J, Dai J, Duan Y et al (2020) Fabrication of PANI–TiO_2/rGO hybrid composites for enhanced photocatalysis of pollutant removal and hydrogen production. Renew Energy 156:1008–1018. https://doi.org/10.1016/j.renene.2020.04.104
147. Kanamarlapudi SLRK, Chintalpudi VK, Muddada S (2018) Application of biosorption for removal of heavy metals from wastewater. Biosorption 69
148. Alireza K, Ali MG (2011) Nanostructured titanium dioxide materials: properties, preparation and applications. World Scientific, Singapore
149. Li X, Teng W, Zhao Q, Wang L (2011) Efficient visible light-induced photoelectrocatalytic degradation of rhodamine B by polyaniline-sensitized TiO_2 nanotube arrays. J Nanopart Res 13:6813–6820
150. Mousli F, Chaouchi A, Hocine S et al (2019) Diazonium-modified TiO_2/polyaniline core/shell nanoparticles. Structural characterization, interfacial aspects and photocatalytic performances. Appl Surf Sci 465:1078–1095
151. Eskizeybek V, Sarı F, Gülce H et al (2012) Preparation of the new polyaniline/ZnO nanocomposite and its photocatalytic activity for degradation of methylene blue and malachite green dyes under UV and natural sun lights irradiations. Appl Catal B 119–120:197–206. https://doi.org/10.1016/j.apcatb.2012.02.034
152. Chowdhury D, Paul A, Chattopadhyay A (2005) Photocatalytic polypyrrole—TiO_2—nanoparticles composite thin film generated at the air–water interface. Langmuir 21:4123–4128

Affiliations

Nirmala Kumari Jangid[1] · Sapana Jadoun[2,3] · Anjali Yadav[1] · Manish Srivastava[1] · Navjeet Kaur[1]

✉ Sapana Jadoun
sjadoun022@gmail.com; sapana@lingaysuniversity.edu.in

[1] Department of Chemistry, Banasthali Vidyapith, Banasthali, Rajasthan 304022, India

[2] Department of Chemistry, School of Basic and Applied Sciences, Lingayas Vidyapeeth, Faridabad 121002, Haryana, India

[3] Department of Chemistry, Jamia Millia Islamia, New Delhi 110025, India